PLOS ONE

Mathematical modelling of tissue growth control by positive and negative feedbacks

Bogdan Kazmierczak[1], **Vitaly Volpert** [2,3]*

1 Institute of Fundamental Technological Research, Polish Academy of Sciences, Warsaw, Poland,
2 Institut Camille Jordan, UMRCNRS, University Lyon 1, Villeurbanne, France, **3** Peoples Friendship University of Russia (RUDN University), Moscow, Russia

* volpert@math.univ-lyon1.fr

Abstract

This study investigates the regulation of tissue growth through mathematical modeling of systemic and local feedback mechanisms. Employing reaction-diffusion equations, the models explore the dynamics of tissue growth, emphasizing endocrine signaling and inter-tissue communication. The analysis identifies critical factors influencing the emergence of spatial structures, bifurcation phenomena, the existence and stability of stationary pulse and wave solutions. It also elucidates mechanisms for achieving coordinated tissue growth. In particular, if negative feedback is sufficiently strong, their final finite size is provided by a stable pulse, otherwise they manifest unlimited growth in the form of a wave. These findings contribute to the theoretical insights into biological processes such as embryogenesis, regeneration, and tumor development, while highlighting the role of feedback systems in maintaining physiological homeostasis.

1 Introduction

1.1 Tissue growth regulation

The proportions of the human body, including the size and relative proportions of different organs, are primarily determined by a combination of genetic factors [1] and biological signaling pathways during growth, development and regeneration [2,3]. Genes play a critical role in determining how organs develop and maintain proper proportions relative to one another. For example, genes regulate the production of growth factors, hormones, and proteins that influence cell growth, organ formation, and the overall shape of the body. Hox genes, in particular, are a set of genes that determine the basic body plan and help control the spatial arrangement of organs and tissues during embryonic development. They ensure that organs form in the correct places and proportions.

Growth factors like fibroblast growth factor (FGF), transforming growth factor (TGF), and insulin-like growth factor (IGF) regulate cell division and growth [4,5]. They ensure that different tissues and organs grow at appropriate rates and stop growing when they reach a certain size. Hormones such as growth hormone (produced by the pituitary gland) and thyroid hormone play critical roles in controlling growth in specific organs and overall body development [6]. For example, during puberty, growth hormone and sex hormones cause rapid growth in bones and muscles. Different organs have intrinsic growth programs that regulate

their size independently to a certain degree. For example, the heart develops and grows at a rate that is proportional to the overall body size to ensure proper circulation [7]. The liver has a remarkable ability to regenerate and maintain its proportional size even if a portion is removed [8]. The body uses feedback mechanisms to regulate growth. As certain tissues grow, signals are sent to stop further growth when a critical size is reached. This prevents organs from growing too large or too small in relation to the rest of the body.

Although genetics plays an important role, environmental factors such as nutrition, physical activity, and exposure to toxins can influence how the body grows and how the organs maintain their proportion [2]. For instance, poor nutrition during childhood can lead to stunted growth and smaller organ size.

In general, a complex interaction between genetic, hormonal, and environmental factors governs the proportionality between different organs of the human body. Considering genetic and environmental factors as given, in this work we will focus on feedback mechanisms and tissue cross-talk based on the exchange of signaling molecules such as hormones and growth factors.

1.2 Tissue cross-talk

Tissue cross-talk refers to the communication and interaction between different tissues within an organism, particularly through signaling molecules like hormones, cytokines, growth factors, and extracellular vesicles. This communication is crucial for coordinating tissue growth, repair, and maintenance in a multicellular organism. During the regulation of tissue growth, these interactions help ensure that different tissues grow in harmony and adapt to changing physiological demands [2].

There are different mechanisms of tissue cross-talk in growth regulation. In the case of paracrine signaling, cells release signaling molecules (such as growth factors) that act on nearby cells. For instance, fibroblasts in connective tissue release growth factors like fibroblast growth factor (FGF), which promote the proliferation of epithelial cells in the skin or other tissues [9]. In endocrine signaling, hormones are released into the bloodstream and affect distant tissues. An example is growth hormone (GH) produced by the pituitary gland, which stimulates growth in bones and muscles [10]. Insulin-like growth factors (IGFs), produced in response to GH, also play a key role in tissue growth regulation [11]. Extracellular vesicles such as exosomes can carry proteins, lipids, and RNA between tissues, allowing them to communicate over long distances. These vesicles can regulate cell proliferation, differentiation, and tissue repair by transferring growth-promoting or inhibitory signals [12].

The immune system is also involved in tissue growth regulation. For example, macrophages and other immune cells release cytokines that promote or inhibit cell proliferation and tissue growth, depending on the context (e.g., during injury repair or in chronic inflammation) [13].

Among key examples of tissue cross-talk in growth regulation we can cite bone-muscle cross-talk [14]. During skeletal growth, there is coordination between bone and muscle tissues. Muscle-derived growth factors, such as myokines, influence bone development, while bone-derived factors, such as osteokines, regulate muscle growth. This interaction is crucial for proper musculoskeletal development and maintaining function throughout life.

Adipose tissue (fat) and muscle also engage in cross-talk through hormones like leptin and adiponectin [15]. Leptin, secreted by fat cells, influences energy metabolism and muscle function, while muscle-derived myokines regulate fat metabolism. This interaction is important in obesity, where dysregulation can lead to abnormal tissue growth and metabolic issues.

In cancer, the cross-talk between tumor cells and surrounding stromal tissue is a key aspect of tumor growth regulation [16]. Stromal cells can secrete growth factors and remodel the ECM to support tumor expansion, while tumor cells can influence the surrounding microenvironment to suppress immune responses or promote angiogenesis.

Tissue cross-talk plays a dynamic role in coordinating the growth and adaptation of different tissues, allowing the organism to maintain a balanced physiological state. When these interactions are disrupted, it can lead to abnormal growth patterns or diseases such as cancer, fibrosis, or tissue degeneration.

1.3 Models of endocrine system and tissue growth control

Endocrine axes govern and regulate the secretion of hormones from different glands through a sequence of signals. They maintain homeostasis, regulate a plethora of physiological processes (e.g. growth and development, reproductive functions), correlate responses of organisms to environmental changes (e.g. adaptation to stress). Endocrine axes rely on negative feedback loops to maintain appropriate balance between levels of different target hormones thus regulating diverse physiological phenomena. We will discuss the biological mechanisms of such feedbacks in Sect 5.

Mathematical models provide indispensable tools to study tissue cross-talk and related time oscillations in neuroendocrinology [17], energy homeostasis [18], stress response [19], and other body systems [20]. One of the first ODE model of growth processes based on negative feedbacks was presented in [21]. This approach is commonly used in more recent works (see, e.g., [22]). Gradient scaling models and temporal dynamics models in the regulation of drosophila wing disk are reviewed in [2,23,24]. Mathematical models of tissue regeneration are presented in [25].

The main difference and the novelty of the present work is that we consider growing tissue as a spatially distributed system. This approach is quite common in tumor growth models, wound healing or morphogenesis (see, e.g., [26]) but there are few spatial models of tissue growth regulation with systemic feedback. We can cite the models of infection progression with a negative feedback by the adaptive immune response [27–29]. From the point of view of modelling and analysis, the interest of such models is that they contain integral terms and represent nonlocal reaction-diffusion equations with some different properties in comparison with the classical reaction-diffusion models.

In the next section, we will develop mathematical models of tissue growth regulation with systemic feedback. We will make abstraction of specific tissues and signaling molecules in order to develop a general framework of such models. Specific tissues and their cross-talk will be studied in the other works. Sect 3 is devoted to differentiation and growth of a single tissue, and Sect 4 to coordinated growth of two tissues. In Sect 5, we discuss different mechanism of tissue growth control in relation to the modelling results, and conclude this paper in the last section.

2 Tissue growth regulation models

In this section, we will derive the tissue growth models, which will be studied in the next sections. We focus on the regulation of tissue growth through endocrine signaling involving another tissue or organ of the body. We begin with growth regulation of a single tissue and continue with the mutual regulation of two growing tissues.

2.1 Endocrine regulation of a single tissue

The cell concentration $u(x,t)$ in the tissue is described by the equation

$$\frac{\partial u}{\partial t} = D\frac{\partial^2 u}{\partial x^2} + F(u, C),$$

(1)

where C is the concentration of some biochemical substance (growth factor, hormone) regulating tissue growth. We take into account random cell motion described by the diffusion term. The function $F(u,C)$ is considered in the form

$$F(u, C) = f_0(C)(a + bu)u(1 - u) - g_0(C)u.$$

(2)

The first term in this function describes cell proliferation rate and the second term cell death. The logistic term $u(1-u)$, commonly used to model tissue growth and cell proliferation, captures the phenomenon of density-dependent proliferation, where cell division slows down as cell density increases. This is a well-established concept both biologically [30–32] and mathematically [33–35].

The extended proliferation term $(a + bu)u(1 - u)$ in tissue growth models introduces density-dependent signaling effects—particularly autocrine and paracrine signaling—which modulate cell division beyond the basic logistic growth. The factor $(a + bu)$ reflects positive feedback where cells stimulate their own proliferation or that of their neighbors through chemical signaling. As such, many cells produce growth factors (e.g., EGF, FGF, TGF-β) that stimulate their own division (autocrine) or that of nearby cells (paracrine). The local concentration of these factors increases with cell density u, hence justifying a term like $(a + bu)$ to represent enhanced division [36–38]. In models of tumor growth or wound healing, the proliferation rate is often modeled as a function of local signal concentration, which in turn depends on u [39]. Models explicitly accounting for autocrine loops introduce proliferation terms with overlinear growth to reflect increasing signaling strength with density [40,41].

The functions $f_0(C)$ and $g_0(C)$ show the dependence of cell proliferation and death on endocrine signaling. Endocrine signaling profoundly influences both cell proliferation and death across tissues by modulating signaling pathways, transcription factors, and feedback loops. This regulation is not only experimentally established but also supported by a range of mathematical models, which help in predicting dynamics under normal and pathological conditions. Hormones produced by endocrine glands travel through the bloodstream and affect target tissues by binding to specific receptors, regulating gene expression, and thereby influencing cell proliferation. As such, estrogens stimulate the proliferation of breast epithelial cells. Estrogen binds to estrogen receptors (ER), leading to activation of genes promoting cell cycle progression [42]. Insulin and IGF-1 promote proliferation in various tissues, including muscle, liver, and even in tumor cells. Insulin-like growth factor 1 (IGF-1) activates PI3K/AKT and MAPK pathways, which promote survival and proliferation [43]. Endocrine factors also regulate programmed cell death, which is crucial for tissue homeostasis. In particular, cortisol (glucocorticoid) induces apoptosis in immune cells such as lymphocytes [44]. This is crucial during inflammation resolution. Thyroid hormones regulate apoptosis during brain development and metamorphosis in amphibians [45]. Endocrine regulation is considered in mathematical models of cancer [46,47], hematopoiesis [48], immune response [49].

Endocrine signaling is characterized by hormones secreted into the bloodstream by endocrine glands (e.g., pituitary, thyroid, adrenal glands) that regulate the activity of distant target tissues. However, the regulation is not unidirectional. There is substantial evidence that

target tissues themselves produce feedback signals, often in proportion to their mass, activity, or functional state, to modulate the upstream endocrine output. This allows the organism to match hormonal stimulation to physiological need. Among many examples of such feedback regulation between the target tissue and endocrine signaling, we can cite hypothalamic-pituitary-endocrine axis [50,51], erythropoiesis regulation [52,53], insulin and glucose homeostasis [54,55], bone mass and FGF23 [56,57], muscle-liver feedback [58,59].

Thus, target tissues often secrete feedback molecules that serve as informative cues about their volume, activity, or functional state. Denote by B its level in the organism. Then

$$\frac{dB}{dt} = k_1 J(u) - \sigma_1 B. \tag{3}$$

Its production rate is proportional to the total tissue volume,

$$J(u) = \int_{-\infty}^{\infty} u(x,t)dx$$

(for the space variable x considered on the whole axis). The second term in the right-hand side of Eq (3) describes its degradation or depletion.

This substance B is transported to another organ or tissue by blood flow and stimulates there production of the endocrine signaling molecule C regulating tissue growth in Eq (1):

$$\frac{dC}{dt} = k_2 B - \sigma_2 C - \sigma_3 J(u) C. \tag{4}$$

Here C is its concentration in the organism (or its level in blood). It acts on the cells of the tissue where its depletion is proportional to the total cell concentration $J(u)$ (Fig 1). Note that the characteristic time scale of hormone distribution by the blood circulation is essentially less than the characteristic time of cell division and tissue growth. Therefore, hormone redistribution is considered as instantaneous, and the process of this redistribution is not considered in the models of tissue growth and regeneration.

Problem (1)-(4) represents a combination of a reaction-diffusion equation for the variable $u(x,t)$ as a function of space and time with ordinary differential equations for $B(t)$ and
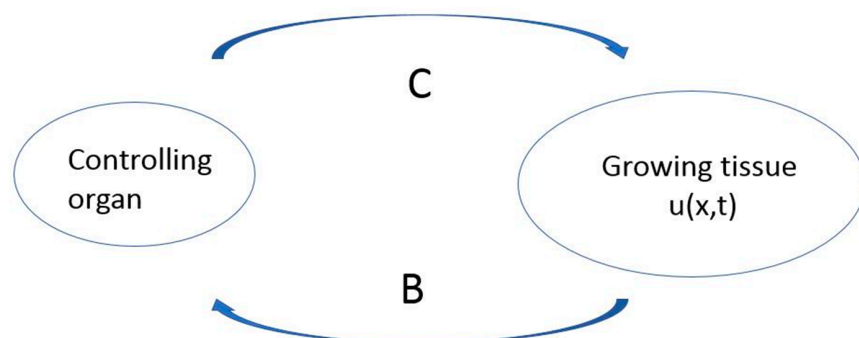
Fig 1. Schematic representation of the model. Growing tissue produces some signaling molecule B with the production rate proportional to the total cell concentration $\int u(x,t)dx$. It is transported by the blood flow to the controlling organ and stimulates there production of a feedback signaling molecule C which can amplify or inhibit tissue growth.

$C(t)$. Eq (1) will be considered either on the whole axis or in a bounded interval with Neumann boundary conditions. Note that all variables in these equations are dimensionless. As such, $u(x,t)$ is the cell concentration, that is the number of cells in unit volume, normalized to its maximal value. Dimensionless equation (1) is obtained from the dimensional equation by division on the maximal cell concentration. Parameter a in this equation has a meaning of cell proliferation rate normalized by the maximal cell concentration, that is, relative increase of cell concentration in a unit volume during a unit time. Parameter b characterizes the influence of cell-cell interaction on their division rate. Diffusion coefficient D has dimension $(s_{un})^2/t_{un}$, where s_{un} is a space unit, t_{un} is a time unit. Functions f and g represent dimensionless rate coefficients. Coefficients $k_1, k_2, \sigma_1, \sigma_2, \sigma_3$ characterize the rates of production or degradation of signaling molecules B and C.

Since production and redistribution of B and C can be considered as fast compared to the cell division and death, we can use a quasi-stationary approximation in Eqs (3), (4) setting zero the time derivatives:

$$B = k_1 J(u)/\sigma_1, \quad C = k_2 B/(\sigma_2 + \sigma_3 J(u)).$$

Therefore,

$$C = \frac{k_1 k_2 J(u)}{\sigma_1(\sigma_2 + \sigma_3 J(u))}$$

can be substituted into Eq (1).

Substituting all these expressions in Eq (1) we obtain the following equation

$$\frac{\partial u}{\partial t} = D\frac{\partial^2 u}{\partial x^2} + f(J(u))(a+bu)u(1-u) - g(J(u))u. \tag{5}$$

All coefficients in this equation are some positive constants. We consider it either on the whole axis or on a bounded interval with no-flux (Neumann) boundary conditions. We will specify the functions $f(C)$ and $g(C)$ below.

2.2 Tissue cross-talk and coordinated growth

Tissue cross-talk refers to the biochemical communication between different tissues via signaling molecules such as cytokines, growth factors, hormones, or extracellular vesicles. This communication is crucial for maintaining homeostasis and coordinating complex physiological processes like development, regeneration, and immune responses. The coordinated growth of tissues via cross-talk ensures that organs develop proportionately and functionally integrate during embryogenesis, wound healing, and disease.

Tissues secrete signaling molecules that act on nearby (paracrine) or distant (endocrine) cells to modulate their behavior, including proliferation and apoptosis. As such, in limb development, mesenchymal and epithelial tissues communicate via Fibroblast Growth Factors (FGFs) and Sonic Hedgehog (Shh). FGFs from the apical ectodermal ridge stimulate mesenchymal proliferation, while Shh from the zone of polarizing activity influences patterning and growth coordination [60].

Tissue cross-talk during organogenesis involves reciprocal signaling loops, ensuring proportional and coordinated organ development. For example, in the liver–pancreas axis, FGF and BMP signals from the cardiac mesoderm and septum transversum mesenchyme guide hepatic specification, and later liver-derived signals modulate pancreatic islet development [61]. In metabolic regulation of adipose–muscle tissue cross-talk, adipose tissue secretes

adipokines (e.g., leptin, adiponectin) and muscle secretes myokines (e.g., IL-6, irisin), which regulate each other's growth and function [58].

In tumors, the tumor microenvironment (fibroblasts, immune cells) and cancer cells engage in cross-talk that regulates tumor cell proliferation and apoptosis. Though pathological, this illustrates the broader principle of cross-tissue signaling influencing growth. In particular, cancer-associated fibroblasts (CAFs) secrete TGF-β, VEGF, and other growth factors that stimulate tumor growth and angiogenesis [62].

In bone marrow–immune system interactions, hematopoietic stem cells (HSCs) in bone marrow receive signals from bone-forming osteoblasts and vice versa. Osteoblasts secrete osteopontin, which affects HSC quiescence and proliferation. This interaction ensures that the expansion of the bone matrix and the replenishment of blood cells are coordinated [63].

Thus, tissue cross-talk via diffusible factors, extracellular vesicles, or direct cell–cell contact ensures synchronized growth by adjusting proliferation/apoptosis rates based on systemic needs, mediating feedback loops during development and regeneration, responding to physiological and pathological stimuli.

We now develop a mathematical model for the description of coordinated growth of two tissues. Consider two tissues with normalized concentrations of cells $u(x,t)$ and $v(x,t)$, respectively. These concentrations are described by the following system of equations:

$$\frac{\partial u}{\partial t} = D\frac{\partial^2 u}{\partial x^2} + f_1(c_1,c_2)(a_1 + b_1 u)u(1-u) - g_1(c_1,c_2)u, \tag{6}$$

$$\frac{\partial v}{\partial t} = D\frac{\partial^2 v}{\partial x^2} + f_2(c_1,c_2)(a_2 + b_2 v)v(1-v) - g_2(c_1,c_2)v. \tag{7}$$

Each of these equations is similar to Eqs (1), (2) described in Sect 2.1. As before, the right-hand side of Eq (6) describes random cell motion, cell proliferation and death. Cell proliferation rate is proportional to their concentration u and to the logistic term $(1-u)$ describing density-dependent proliferation. The factor $(a_1 + b_1 u)$ shows that proliferation rate increases with u due to local cell-cell communication. Finally, the factor $f_1(c_1,c_2)$ shows how the proliferation rate depends on the cytokines produced by both tissues. The properties of this and other functions will be specified below. Cell death rate also depends on the concentrations of cytokines through the function $g_1(c_1,c_2)$. A similar equation is considered for the concentration v.

According to the biological data on tissue cross-talk described above, each tissue produces a signaling molecule acting on the rates of cell proliferation and death. Their concentrations are described by the equations:

$$\frac{dc_1}{dt} = k_{11}J_1(u) - k_{12}c_1, \tag{8}$$

$$\frac{dc_2}{dt} = k_{21}J_2(v) - k_{22}c_2. \tag{9}$$

Here

$$J_1(u) = \int_\infty^\infty u(x,t)dx, \quad J_2(v) = \int_\infty^\infty v(x,t)dx$$

are the total tissue volumes (for the problem considered on the whole axis). In order to simplify the model, we consider that the same molecule c_1 (c_2) produced by the first (second) tissue participates in the regulation of both tissues. In a more general case, these signaling molecules can be different.

There are different cases according to the form of the functions f_i, g_i:

- Cell death is promoted by cells of the same type and down-regulated by cells of the different type, cell proliferation is independent of them,

$$g_1(c_1, c_2) = \frac{r_1 + r_2 c_1}{r_3 + r_4 c_2}, \quad g_2(c_1, c_2) = \frac{s_1 + s_2 c_2}{s_3 + s_4 c_1}, \quad f_i \equiv 1, \quad i = 1, 2. \tag{10}$$

- Cell proliferation is promoted by cells of the different type and down-regulated by cells of the same type, cell death is independent of them,

$$f_1(c_1, c_2) = \frac{r_1 + r_2 c_2}{r_3 + r_4 c_1}, \quad f_2(c_1, c_2) = \frac{s_1 + s_2 c_1}{s_3 + s_4 c_2}, \quad g_i \equiv 1, \quad i = 1, 2. \tag{11}$$

- Cell death and proliferation can depend on signaling with c_1 and c_2.

Summarizing these different conditions, we assume that each tissue down-regulates its own growth through a negative feedback determined by the tissue volume. On the other hand, each tissue promotes growth of the other one (Fig 2). These assumptions are confirmed by some biological observations [64]. Moreover, according to this work, cessation of developmental growth is, in the final stages, due more to an increase in the rate of cell loss than to a reduction in the rate of cell proliferation.

3 Differentiation and growth of a single tissue

We consider the following equation for the concentration of tissue cells $u(x,t)$:

$$\frac{\partial u}{\partial t} = D \frac{\partial^2 u}{\partial x^2} + f(c)(a + bu)u(1 - u) - g(c)u. \tag{1}$$
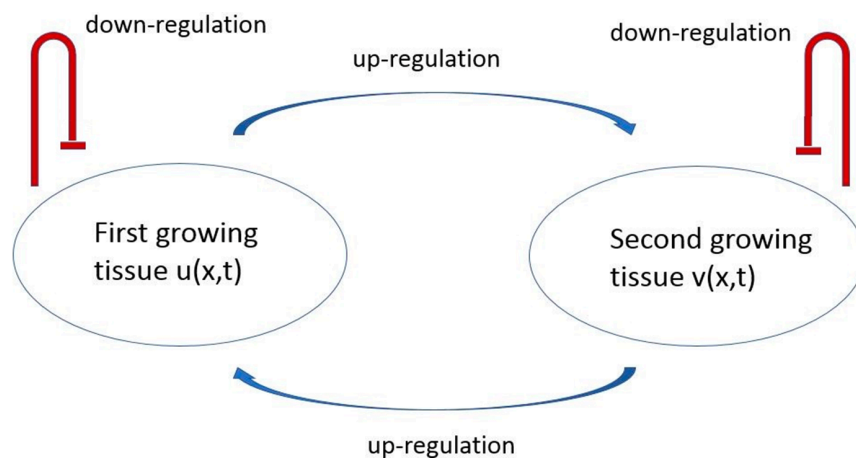
Fig 2. Schematic representation of the model for the coordinated growth of two tissues. Each of them down-regulates its own growth and up-regulates growth of the other one.

The diffusion term in the right-hand side of this equation describes random cell motion, the next term characterizes cell proliferation and the last term their death. The cell proliferation rate is considered in logistic form taking into account the decrease and arrest of the proliferation rate for the dimensionless cell concentration $u = 1$. On the other hand, cell proliferation increase due local cell-cell communication and paracrine signaling is described by the factor $(a + bu)$. Finally, endocrine signaling on cell proliferation is described by the function $f(c)$. Its influence on cell death is taken into account through the function $g(c)$. These functions will be specified below. We recall that, according to Eq. (5), $c = \int_{-\infty}^{\infty} u(x,t)\,dx$ for the problem on the whole axis. For the problem on a bounded interval, the integral is taken with respect to this interval.

3.1 Bifurcation of spatially distributed solutions

For simplicity of calculations, we suppose that $f(c) \equiv 1$. Let $g(c)$ be a non-negative continuous function defined for $c \geq 0$. The particular case $g(c) = c$ is studied in [65].

Consider Eq (1) on a bounded interval [0,L] with the Neumann boundary conditions:

$$x = 0, L : \frac{\partial u}{\partial x} = 0. \tag{2}$$

For a positive homogeneous in space stationary solution of problem (1), (2), $J(u) = Lu$, and it can be found as a solution of the equation

$$(a + bu)(1 - u) = g(Lu). \tag{3}$$

Suppose that such solution exists and denote it by u_0.

We linearize Eq (1) about this solution and obtain the eigenvalue problem:

$$Dv'' + (a - 2au_0 + 2bu_0 - 3bu_0^2)v - g(Lu_0)v - g'(Lu_0)u_0 J(v) = \lambda v, \tag{4}$$

or, taking into account (3),

$$Dv'' + (-a + b - 2bu_0)u_0 v - g'(Lu_0)u_0 J(v) = \lambda v \tag{5}$$

with the boundary conditions

$$v'(0) = v'(L) = 0. \tag{6}$$

We consider the eigenfunctions

$$v_n(x) = \cos\left(\frac{\pi n}{L} x\right), \quad n = 0, 1, 2, \dots$$

and determine the corresponding eigenvalues:

$$\lambda_0 = (b - a - 2bu_0)u_0 - g'(Lu_0)Lu_0, \quad \lambda_n = (b - a - 2bu_0)u_0 - D\left(\frac{\pi n}{L}\right)^2, \quad n = 1, 2, \dots \tag{7}$$

The properties of the eigenvalues are formulated in the following theorem.

Theorem 3.1. *Suppose that*

$$g'(Lu_0) > 0, \quad 0 < u_0 < \frac{b-a}{2b}, \tag{8}$$

and

$$D < \frac{1}{\pi^2} \min \left((b-a-2bu_0)u_0 L^2, g'(Lu_0)L^3 u_0 \right).$$

*Then λ_1 is a positive eigenvalue with the maximal real part,*

$$\lambda_1 > 0, \quad \lambda_1 > \lambda_0, \quad \lambda_1 > \lambda_n, \quad n = 2, 3, \dots$$

The assertion of the theorem follows directly from (7). It means that the loss of stability of the homogeneous in space solution occurs with a space-dependent eigenfunction (see, e.g., [66], p. 528). Therefore, this instability leads to the bifurcation of a space-dependent solution. This is different for the equation without the integral term. In this case, $\lambda_0 > \lambda_1$, and spatial structures do not emerge (see more details in [65]).

Note that if $b > a$ and $g(u) = kg_0(u)$, where $g_0(u)$ is a positive growing function such that $g_0(0) = 0$, then the conditions of the theorem are satisfied for all k sufficiently large and all D sufficiently small.

Example. Let $g(J) = kJ$ and $a = 0$. Then the instability conditions can be written in the following form [65]: $b/(2k) < L < b/k$, $D < L^2(2kL - b)(b - kL)/(b\pi^2)$. Note that the instability emerges for the values of L in some bounded interval. This is different in comparison with the Turing instability for which L should only exceed some minimal value.

Some examples of solutions bifurcating from the spatially uniform solution are shown in Fig 3. Let us note that for an asymmetric initial condition, solution converges to the half-pulse solution, while for a symmetric initial condition to the whole pulse solution. Since the initial condition is symmetric, it is orthogonal to the first eigenfunction, and the solution remains in this subspace. Since the second eigenvalue λ_2 is also positive for these values of parameters, the solution converges to a symmetric pulse solution.
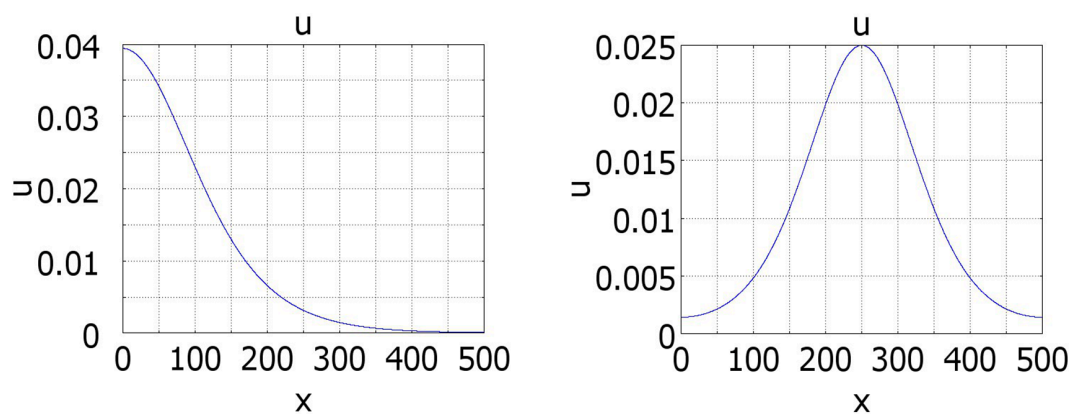
Fig 3. Numerical simulations of equation (1) with $f(J) \equiv 1$ and $g(J) = kJ$, $a = 0.5$, $b = 1$, $k = 0.1$. Left: $D = 50$, the initial data are: $0.1H(x–250–50)H(250–x)$. Right: $D = 20$, the initial data are: $0.1H(x – 250 – 25)H(250 + 25 – x)$.

Taking into account different possible applications and wide variation of biological parameters, the choice of parameter values is motivated by the purposes of modelling, such as the conditions of the emergence of spatial structures and different regimes of tissue growth.

3.2 Existence and stability of pulses on the whole axis

We consider the stationary equation

$$Dw'' + (a + bw)w(1 - w) - g(J(w))w = 0 \tag{9}$$

on the whole axis. We look for a positive solution of this equation vanishing at infinity,

$$w(\pm\infty) = 0. \tag{10}$$

Consider the auxiliary problem

$$Dw'' + (a + bw)w(1 - w) - hw = 0, \quad w(\pm\infty) = 0, \quad w(x) > 0, \quad x \in \mathbb{R} \tag{11}$$

and denote by $w_h(x)$ its positive solution. Then solution of the equation

$$g(J(w_h)) = h \tag{12}$$

provides a solution of problem (9), (10).

Problem (11) has a solution if $b > a > 0$ and $a < h < h_*$, where $h_* > a$ is a positive number which can be determined analytically (see p. 4 in [65]). Moreover,

$$J(w_h) \to \begin{cases} 0 & , & h \to a \\ \infty & , & h \to h_* \end{cases} .$$

We can now formulate the existence result.

Theorem 3.2. *Suppose that $b > a > 0$, $g(0) < a, g(\infty) > h*$ or $g(0) > a, g(\infty) < h*$. Then problem (9), (10) has a positive solution.*

Consider some examples.

Examples. If $g(c) = kc^n$ with some positive k and n, then the conditions of the theorem are satisfied. They are also satisfied for negative n, but these two cases are different. Introduce the function $F(h) = g(J(w_h)) - h$ and consider the equation $F(h) = 0$. If it has a single solution h_0, then $F'(h_0) \geq 0$ for $n > 0$ and $F'(h_0) \leq 0$ for $n < 0$. This is related to stability and bifurcations of solutions. If $n = 0$, then Eq (9) is independent of $J(u)$ and the pulse is unstable [67].

**Remark.** If the function $f(J)$ is not constant, then equation

$$Dw'' + f(J(w))(a + bw)w(1 - w) - g(J(w))w = 0 \tag{13}$$

can be reduced to an equation similar to (9) by the introduction of a new function $v(x\sqrt{f(J(w))}) = w(x)$.
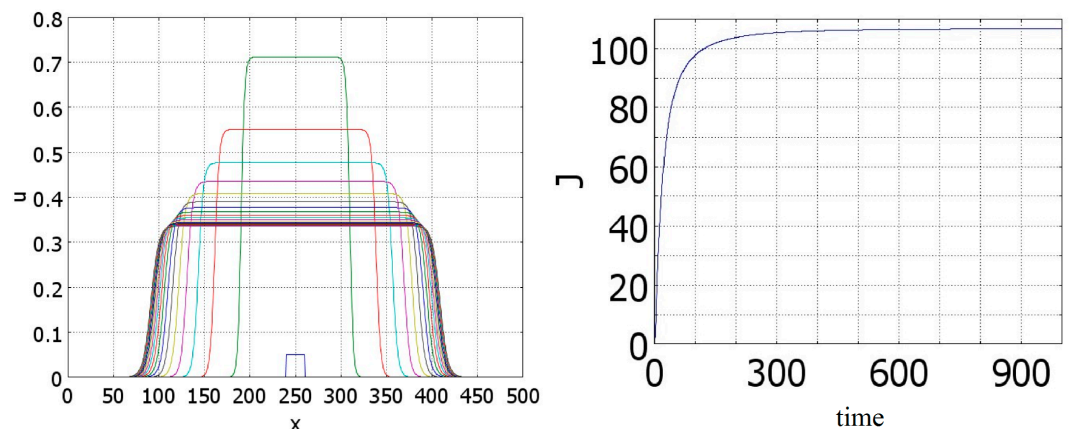
3.3 Numerical simulations

Some examples of numerical simulations are shown in Figs 4 and 5. If conditions of Theorem 2.2 are satisfied, then there exists a stationary pulse solution. For the values of parameters in Figs 4 (left), it is stable, and the solution of Eq (1) converges to it. On the contrary, for the values of parameters in Figs 4 (right), the pulse does not exist, and we observe wave propagation.

Under the conditions of the theorem, if solution h of Eq (12) is sufficiently close to the value h_*, then the pulse solution exists, it is wide and top-flat (Fig 5, left). The figure shows convergence of solution of the initial boundary value problem to the stationary pulse solution. Let us note that the initial condition is small. Contrary to the conventional bistable reaction-diffusion equation, here the solution can grow even for any small initial condition. In fact, the presence of the integral in the equation changes its type from the monostable case for small $J(u)$ to the bistable case for large values. Thus, solution grows, takes the form of a flat
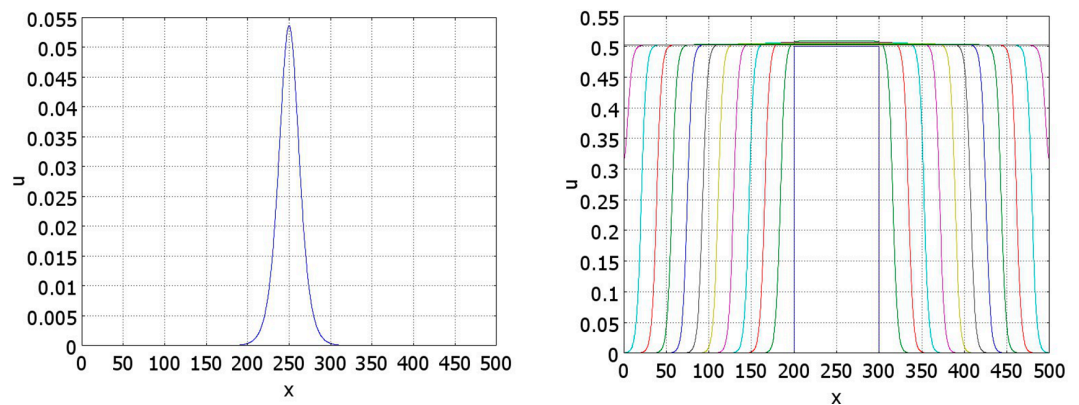
Fig 4. Numerical simulations of Eq (1) with $f(J) \equiv 1$ and $g(J) = k_1 + k_2 J/(1 + J)$, $a = 0.5$, $b = 1$. Left: solution converges to a stationary pulse, $k_1 = 0.2$, $k_2 = 0.5$, $J = 1.7237$, $t = 1200$. Right: solution propagates as a wave, $k_1 = 0.2$, $k_2 = 0.3$, $t = 0, 50, 100, ..., 600$.

https://doi.org/10.1371/journal.pone.0319120.g004

Fig 5. Numerical simulations of Eq (1) with $f(J) \equiv 1$ and $g(J) = (k_1 + k_2 exp(0.05J)/(100 + exp(0.05J)))$, $a = 0.5$, $b = 1$, $k_1 = 0.05$, $k_2 = 0.75$. The left panel shows convergence of solution to the stationary pulse, $t = 0, 50, 100, ..., 1000$. The corresponding function $J(u)(t)$ is shown in the right panel.

https://doi.org/10.1371/journal.pone.0319120.g005

pulse, then decreases its height and increases its width. The right panel in this figure shows the convergence of $J(u)(t)$ to its limiting value.

The decrease of the plateau value in Fig 5 is determined by the density-dependent cell proliferation. If the decrease of the proliferation rate is faster, then the decrease of the plateau value is not so essential. For example, if we impose the condition that cells stop proliferation if they touch each other and proliferate otherwise, then for a uniform cell distribution, proliferation rate becomes $(a + bu)u\phi(u)$, where $\phi(u) = \phi_0 > 0$ for $0 \leq u < 1$ and $\phi(1) = 0$. An example of such simulation is presented in Fig 6.

4 Coordinated growth of two tissues

Growth of different tissues during the development of the organism is precisely coordinated. In this section, we study simultaneous growth of two tissues which exchange signals and influence their respective growth rates and final sizes.
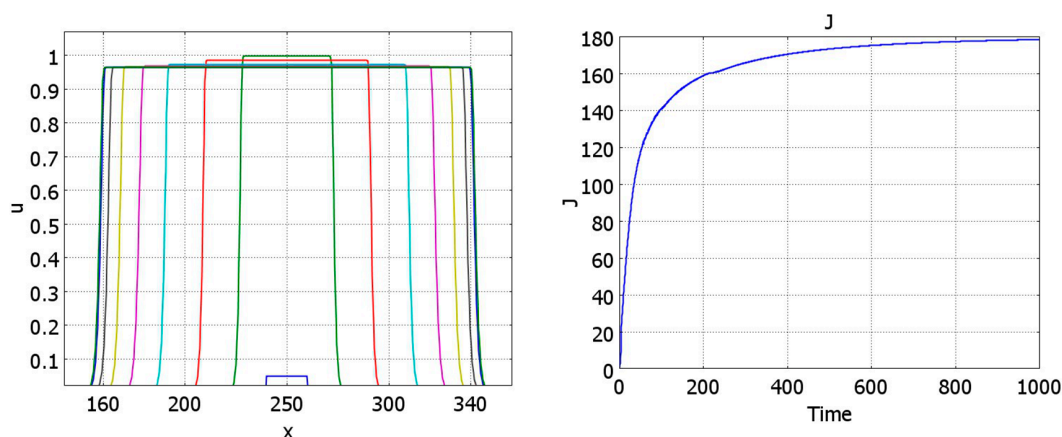
4.1 Existence of pulses

We consider quasi-stationary approximations in Eqs (8), (9). Then

$$c_1 = k_{11}J_1(u)/k_{12}, \quad c_2 = k_{21}J_2(v)/k_{22}, \tag{1}$$

and Eqs (6), (7) become as follows:

$$\frac{\partial u}{\partial t} = D\frac{\partial^2 u}{\partial x^2} + (a_1 + b_1 u)u(1 - u) - \frac{r_1 + k_1 J_1(u)}{r_2 + k_2 J_2(v)}u, \tag{2}$$

$$\frac{\partial v}{\partial t} = D\frac{\partial^2 v}{\partial x^2} + (a_2 + b_2 v)v(1 - v) - \frac{s_1 + n_1 J_2(v)}{s_2 + n_2 J_1(u)}v, \tag{3}$$

Fig 6. Numerical simulations of Eq (1) with $f(J) \equiv 1$ and $g(J) = (k_1 + k_2 exp(0.05J)/(100 + exp(0.05J)))$, $a = 0.5$, $b = 1$, $k_1 = 0.05$, $k_2 = 1.1$. The left panel shows convergence of solution to the stationary pulse, $t = 0, 12.5, 25, 50, 100, 200, 400, 800, 1000$. The corresponding function $J(u)(t)$ is shown in the right panel. The proliferation rate is given by the function $(a + bu)u(1 - u^{100}/(u^{100} + 0.1))$ with the density dependence approximating a step-wise constant function $\phi(u)$.

where

$$k_1 = \frac{k_{11}r_2}{k_{12}}, \quad k_1 = \frac{k_{21}r_4}{k_{22}}, \quad n_1 = \frac{k_{11}s_2}{k_{12}}, \quad n_2 = \frac{k_{21}s_4}{k_{22}}.$$

We look for a positive stationary solution $w(x), z(x)$ of this system of equations on the whole axis:

$$Dw'' + (a_1 + b_1 w)w(1-w) - \frac{r_1 + k_1 J_1(w)}{r_2 + k_2 J_2(z)}\, w = 0, \tag{4}$$

$$Dz'' + (a_2 + b_2 z)z(1-z) - \frac{s_1 + n_1 J_2(z)}{s_2 + n_2 J_1(w)}\, z = 0 \tag{5}$$

vanishing at infinity:

$$w(\pm\infty) = 0, \quad z(\pm\infty) = 0. \tag{6}$$

Consider the auxiliary problem

$$Dw'' + (a_1 + b_1 w)w(1-w) - pw = 0, \tag{7}$$

$$Dz'' + (a_2 + b_2 z)z(1-z) - qz = 0, \tag{8}$$

$$w(\pm\infty) = 0, \quad z(\pm\infty) = 0, \tag{9}$$

and denote its solution by $(w_p(x), z_q(x))$. This solution provides a solution of problem (4)-(6) if

$$\frac{r_1 + k_1 J_1(w_p)}{r_2 + k_2 J_2(z_q)} = p \tag{10}$$

and

$$\frac{s_1 + n_1 J_2(z_q)}{s_2 + n_2 J_1(w_p)} = q. \tag{11}$$

Lemma 4.1. *The function $J_1(w_p)$ is positive and continuous in the interval $a_1 < p < p_*$ for some $p_* > a_1$, $J_1(w_p) = 0$ for $p = a_1$, and $J_1(w_p) \to \infty$ as $p \to p_*$. The function $J_2(z_q)$ is positive and continuous in the interval $a_2 < q < q_*$ for some $q_* > a_2$, $J_2(z_q) = 0$ for $q = a_2$, and $J_2(z_q) \to \infty$ as $q \to q_*$.*

Proof. By definition, $w_p(x)$ is a positive solution of Eq (7) vanishing at infinity. It is independent of q. The function $F_h(w) = (a + bw)w(1-w) - hw$ can have from one to three non-negative zeros. Suppose that there are three of them. This is the case if

$$b > a, \quad a < h < \frac{(a+b)^2}{4b}\,.$$

Denote by $w_0(h)$ the maximal solution of the equation $F_h(w) = 0$. It is known that Eq (7) has a positive solution $w_h(x)$ vanishing at infinity if and only if $\int_0^{w_0(h)} F_h(w)dw > 0$. This inequality holds for $a < h < h_* = (2(a+b)^2 + ab)/(9b)$.

Denote $w_m(h) = \max_{x\in\mathbb{R}} w_h(x)$. Then $w_m(h) < w_0(h)$. If $h \nearrow h_*$, then $w_m(h) \nearrow w_0(h)$, $w_h(x) \to w_0(h)$ uniformly in x on every bounded interval and, consequently, $J_1(w_h) \to \infty$ (see [65] for more detail).

Next, suppose that $h \searrow a$ and set $h = a + \epsilon$. Then Eq (7) can be written as follows:

$$Dw'' + (b-a)w^2 - bw^3 - \epsilon w = 0. \tag{12}$$

Let us introduce a new function $u(y)$ by the equality $w(x) = \epsilon v(\sqrt{\epsilon}x)$. Then it satisfies the equation

$$Dv'' + (b-a)v^2 - v - b\epsilon v^3 = 0, \tag{13}$$

where prime denotes the derivative with respect to y. If $b > a$ and ϵ is sufficiently small, then this equation has a positive solution $v_\epsilon(y)$ vanishing at infinity. Then

$$J_1(w_h) = \int_{-\infty}^{\infty} w_h(x)dx = \epsilon \int_{-\infty}^{\infty} v_\epsilon(\sqrt{\epsilon}x)dx = \sqrt{\epsilon} \int_{-\infty}^{\infty} v_\epsilon(y)dy \sim \sqrt{\epsilon} \int_{-\infty}^{\infty} v_0(y)dy \to 0$$

as $\epsilon \to 0$.

The second part of the lemma for $J_2(w_q)$ can be proved similarly. The lemma is proved.

Lemma 4.2. *Suppose that system* (10), (11) *has a solution for* $a_1 < p < p_*$, $a_2 < q < q_*$ *in some parameter range. Then* $J_1(w_p) \to \infty$ *if and only if* $J_2(z_q) \to \infty$.

Proof. Suppose that $J_1(w_p) \to \infty$ but $J_2(z_q)$ remains bounded. Then the left-hand side of equality (10) tends to infinity, while the right-hand side remain bounded since $a_1 < p < p_*$. The second case is proved similarly. The lemma is proved.

Lemma 4.3. If

$$\frac{k_1 n_1}{k_2 n_2} \neq p_* q_*, \tag{14}$$

then for p and q satisfying (10), (11), convergence $J_1(w_p) \to \infty$, $J_2(z_q) \to \infty$ does not hold.

Proof. If this convergence occurs, then $p \to p_*$, $q \to q_*$. From Eqs (10), (11) we obtain

$$\frac{r_1 + k_1 J_1(w_p)}{r_2 + k_2 J_2(z_q)} \to p_*, \quad \frac{s_1 + n_1 J_2(z_q)}{s_2 + n_2 J_1(w_p)} \to q_*.$$

Multiplying these equations, we get

$$\frac{r_1 + k_1 J_1(w_p)}{r_2 + k_2 J_2(z_q)} \cdot \frac{s_1 + n_1 J_2(z_q)}{s_2 + n_2 J_1(w_p)} \to p_* q_*.$$

The expression in the left-hand side converges to $k_1 n_1/(k_2 n_2)$. This contradiction proves the lemma.

We begin the analysis of the existence of solutions of system of (10), (11) with the case $r_1 = r_2 = s_1 = s_2 = 0$. Then, multiplying these equations, we obtain $pq = \kappa$, where $\kappa = k_1 n_1/(k_2 n_2)$. The function $h_2(p) = J_2(z_{\kappa/p})$ is defined on the interval $a_2 < \kappa/p < q_*$ or $\kappa/q_* < p < \kappa/a_2$. Together with the function $h_1(p) = J_1(w_p)$, they are defined on the intersection of the intervals

$$I = [a_1, p_*) \cap (\kappa/q_*, \kappa/a_2].$$

We recall that $h_1(a_1) = 0, h_1(p_*) = \infty, h_2(\kappa/q_*) = \infty, h_2(\kappa/a_2) = 0$, and these functions are positive inside their intervals of definition.

Assume that $\kappa/q_* < p_*$ and consider the function

$$H(p) = \frac{k_1 h_1(p)}{k_2 h_2(p)}, \quad p_1 = \max(a_1, \kappa/q_*) < p < \min(p_*, \kappa/a_2) = p_2.$$

Since $h_1(a_1) = 0$ and $h_2(\kappa/q_*) = \infty$, then $H(p_1) = 0$. Next, equalities $h_1(p_*) = \infty$ and $h_2(\kappa/a_2) = 0$ implies that $H(p_2) = \infty$. Hence, equation $H(p) = p$ (equivalent to Eq (10)) has a solution in this interval. We proved the following result.

Proposition 4.4. *Suppose that $r_1 = r_2 = s_1 = s_2 = 0$ and*

$$\frac{k_1 n_1}{k_2 n_2} < p_* q_*. \tag{15}$$

Then problem (4)-(6) has a positive solution. If the inequality is opposite, such solution does not exist.

We will now consider the case without the assumption that some coefficients vanish.

Theorem 4.5. *If $r_1/r_2 < a_1, s_1/s_2 < a_2$ and*

$$\frac{k_1 n_1}{k_2 n_2} > p_* q_*, \tag{16}$$

then problem (4)-(6) has a positive solution.

Proof. If $r_1/r_2 < a_1$, then Eq (10) with respect to p has a solution in the interval (a_1, p_*) for any $q \in [a_2, q_*)$ fixed. Indeed, for $p = a_1, J_1(w_p) = 0, J_2(w_q) \geq 0$, and

$$\frac{r_1 + k_1 J_1(w_p)}{r_2 + k_2 J_2(z_q)} \leq \frac{r_1}{r_2} < a_1 = p.$$

On the other hand, $J_1(w_p) \to \infty$ as $p \to p_*$, and the last inequality becomes opposite for p sufficiently close to p_*. Therefore, Eq (10) has a solution for some intermediate value of p. Denote it by $S(q)$. Then, $S(a_2) > a_1, S(q) \to p_*$ as $q \to q_*$.

Similarly, If $s_1/s_2 < a_2$, then Eq (11) with respect to q has a solution in the interval (a_2, q_*) for any $p \in [a_1, p_*)$. We denote it by $T(p)$, and $T(a_1) > a_2, T(p) \to q_*$ as $p \to p_*$.

We need to verify that the curve $p = S(q)$ and $q = T(p)$ intersect for some $a_2 < q < q_*, a_1 < p < p_*$. This point of intersection provides solution of system (10), (11) and, consequently, of problem (4)-(6). We will show that condition (16) implies that the curve $p = S(q)$ is above $q = T(p)$ in some vicinity of the point (p_*, q_*) (Fig 7). Then the curves intersect inside the rectangle.

We consider the inverse function $q = R(p)$ to the function $p = S(q)$. For simplicity of notation, set

$$f(p) = J_1(w_p), \quad g_1(p) = J_2(w_q) \text{ for } q = R(p), \quad g_2(p) = J_2(w_q) \text{ for } q = T(p).$$
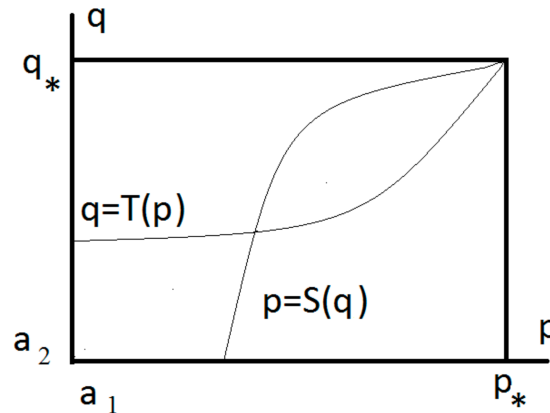
Fig 7. Schematic representation of the curves $p = S(q)$ and $q = T(p)$ on the (p,q)-plane. The former starts at the lower boundary of the domain and tends to the point (p_*, q_*). The latter starts at the left boundary and tends to the same point. If the first curve is above the second curve near this point, as shown in the theorem, they have a point of intersection inside the domain.

Then Eqs (10), (11) become as follows:

$$\frac{r_1 + k_1 f(p)}{r_2 + k_2 g_1(p)} = p, \quad \frac{s_1 + n_1 g_2(p)}{s_2 + n_2 f(p)} = T(p).$$

We obtain from these equations:

$$f(p) = \frac{1}{k_1} \left(r_2 p - r_1 + k_2 p g_1(p) \right), \quad f(p) T(p) = \frac{1}{n_2} \left(s_1 + n_1 g_2(p) - s_2 T(p) \right).$$

Multiplying the first equation by $T(p)$ and equating the right-hand sides, we get the equality:

$$g_1(p) = \alpha(p) g_2(p) + \beta(p), \tag{17}$$

where

$$\alpha(p) = \frac{k_1 n_1}{k_2 n_2 p T(p)}, \quad \beta(p) = \frac{k_1}{k_2 n_2 p T(p)} (s_1 - s_2 T(p)) - \frac{1}{k_2 p} (r_2 p - r_1).$$

Since $p < p_*$, $T(p) < q_*$, then by virtue of condition (16),

$$\alpha(p) = \frac{k_1 n_1}{k_2 n_2 p T(p)} > \frac{k_1 n_1}{k_2 n_2 p_* q_*} > 1.$$

Furthermore, $|\beta(p)| \leq M$, where M is some positive constant independent of p.

Eq (17) implies that $g_1(p) > g_2(p)$ for p sufficiently close to p_*. Indeed, if $g_1(p_i) \leq g_2(p_i)$ for some sequence p_i such that $p_i \nearrow p_*$, then from (17),

$$1 = \alpha(p_i) \frac{g_2(p_i)}{g_1(p_i)} + \frac{\beta(p_i)}{g_1(p_i)} > \frac{k_1 n_1}{k_2 n_2 p_* q_*} - \frac{M}{g_1(p_i)}.$$

Since the first term in the right-hand side of this inequality is larger than 1, and the second one converges to 0, we obtain a contradiction.

Thus, we proved that

$$J_2(w_{R(p)}) > J_2(w_{T(p)}) \ \text{for} \ p \ \text{sufficiently} \quad \text{close} \quad \text{to} \ p_*. \tag{18}$$

If $J_2(w_q)$ is a monotone function of q for q sufficiently close to q_*, then we conclude that $R(p) > T(p)$.

Monotonicity of $J_2(w_q)$ is not needed if we want to verify that $R(p_0) > T(p_0)$ for some p_0. This is sufficient for the intersection of the curves and for the existence of solution. We take a value q_0 of $J_2(w_q)$ for which $J_2(w_q) < J_2(w_{q_0})$ if $q < q_0$. Existence of such q_0 follows from the fact that $J_2(w_q)$ tends to infinity. Then for any q_1 such that $J_2(w_{q_1}) > J_2(w_{q_0})$ it follows that $q_1 > q_0$. We choose p_0 such that $q_0 = T(p_0)$. It follows from (18) that $J_2(w_{R(p_0)}) > J_2(w_{T(p_0)})$. Then $R(p_0) > T(p_0)$.

4.2 Existence of waves

System of Eqs (2), (3) cannot have travelling wave solutions with one of the limits at infinity different from zero since the integrals $J_1(u)$, $J_2(v)$ are not defined in this case. Instead of travelling waves in the classical definition, we will consider the solution of the Cauchy problem converging to two waves moving in the opposite directions, one to minus infinity, another one to plus infinity. In this case, the integrals are well defined. Let us proceed to the description of such solutions and to the conditions of their existence.

Consider the equations

$$\frac{\partial u}{\partial t} = D\frac{\partial^2 u}{\partial x^2} + (a_1 + b_1 u)u(1 - u) - Pu, \tag{19}$$

$$\frac{\partial v}{\partial t} = D\frac{\partial^2 v}{\partial x^2} + (a_2 + b_2 v)v(1 - v) - Qv, \tag{20}$$

where P and Q are some positive constants. If

$$b_i > a_i, \ i = 1, 2, \quad a_1 < P < \frac{(a_1 + b_1)^2}{4b_1}, \quad a_2 < Q < \frac{(a_2 + b_2)^2}{4b_2}, \tag{21}$$

then these are bistable equations. In this case, each of the equations

$$(a_1 + b_1 u)u(1 - u) = Pu, \quad (a_2 + b_2 v)v(1 - v) = Qv$$

has three non-negative solutions, $0, u_1, u_2$ and $0, v_1, v_2$. Eqs (19), (20) have travelling wave solutions with the limits $[0, u_2]$ and $[0, v_2]$. Moreover, there are some values $p_* > a_1$ and $q_* > a_2$ (the same as in Lemma 4.1) such that the inequalities

$$a_1 < P < p_*, \quad a_2 < Q < q_* \tag{22}$$

provide the positivity of the wave speeds. Denote the wave speeds by c_1 and c_2, respectively. If $0 < P < a_1$, then the corresponding equation is monostable, the wave still exists, and we denote by c_1 the minimal wave speed. Similarly, if $0 < Q < a_2$, c_2 is the minimal wave speed for the second equation.

Consider the solution $u(x,t)$ of the Cauchy problem for Eq (19) with a sufficiently large initial condition $u(x,0)$ vanishing at infinity, $u(x,0) \to 0$ as $x \pm \infty$. Then this solution approaches two waves propagating in the opposite directions and $u(x,t) \to u_2$ as $t \to \infty$ uniformly on every bounded interval. Therefore, $J_1(u) \sim 2u_2c_1t$ as $t \to \infty$. Similarly for Eq (20), $J_2(v) \sim 2v_2c_2t$ as $t \to \infty$. We call such solutions expanding wave solutions. We have

$$\frac{r_1 + k_1 J_1(u)}{r_2 + k_2 J_2(v)} \sim \frac{k_1 J_1(u)}{k_2 J_2(v)} \to \frac{k_1 c_1 u_2}{k_2 c_2 v_2} , \quad t \to \infty,$$

$$\frac{s_1 + n_1 J_2(v)}{s_2 + n_2 J_1(u)} \sim \frac{n_1 J_2(v)}{n_2 J_1(u)} \to \frac{n_1 c_2 v_2}{n_2 c_1 u_2} , \quad t \to \infty.$$

System (2), (3) can be reduced asymptotically for large time to system (19), (20) if the following relations are satisfied:

$$\frac{k_1 c_1(P) u_2(P)}{k_2 c_2(Q) v_2(Q)} = P, \quad \frac{n_1 c_2(Q) v_2(Q)}{n_2 c_1(P) u_2(P)} = Q. \tag{23}$$

We take into account here that c_1 and u_2 depend on P, c_2 and v_2 depend on Q, Multiplying these two equalities, we obtain

$$P = \frac{k_1 n_1}{k_2 n_2} \frac{1}{Q} .$$

Since $Q \in (0, q_*)$, then

$$\frac{k_1 n_1}{k_2 n_2} \frac{1}{q_*} < P < \infty.$$

On the other hand, P is defined in the interval $(0, p_*)$. These two intervals intersect if

$$p_* q_* > \frac{k_1 n_1}{k_2 n_2}. \tag{24}$$

It is the same condition as in Proposition 4.4 for the existence of pulses. Assuming that it is satisfied, we consider the equation

$$F(P) \equiv \frac{k_1 c_1(P) u_2(P)}{k_2 c_2(Q) v_2(Q)} = P \tag{25}$$

with respect to P, where

$$Q = \frac{k_1 n_1}{k_2 n_2} \frac{1}{P}, \quad p_0 \equiv \frac{k_1 n_1}{k_2 n_2} \frac{1}{q_*} \leq P \leq p_*.$$

Note that $c_1(p_0) > 0, c_1(p_*) = 0$. Moreover, if $P = p_0$, then $Q = q*$, and $c(Q) = 0$. If $P = p_*$, then $Q < q_*$, and $c(Q) > 0$. Therefore $F(p_0) = \infty$, $F(p_*) = 0$. Moreover, functions $u_2(P)$ and $v_2(Q)$ are bounded from above and from below by some positive constants. Therefore, Eq (25) has a solution. We proved the following theorem.

Theorem 4.6 *If system of Eqs (2), (3) has an expanding wave solution, then inequality (24) is satisfied.*

This assertion does not give sufficient conditions of the existence of such solutions. However, for constant P and Q such solutions do exist. Their existence can be proved for time-dependent P and Q converging to some limits. So, we can expect existence of such solutions for the coupled problem (2), (3).

Conditions of Theorem 4.5 exclude the existence of such solutions, while conditions of Proposition 4.4 admit them. Combining these results with the results of numerical simulations discussed below, we can conclude that waves with positive speeds (Theorem 4.6) exist together with unstable pulses (provided by Proposition 4.4), but not with stable pulses. This is similar for the scalar equation and monotone systems for which unstable pulses exist if and only if the wave speed is positive [68]. Stable pulses do not exist for the scalar equations and monotone systems [67].

The results on tissue growth can be summarized in terms of the non-dimensional parameter

$$S = \frac{k_1 n_1}{k_2 n_2 p_* q_*}$$

characterizing the strength of the feedback. If $S>1$, then the solutions converge to a stable pulse. If the inequality is opposite, they propagate as a wave.

4.3 Numerical simulations

According to the analytical results presented above, inequality

$$\frac{k_1 n_1}{k_2 n_2} < p_* q_* \quad \text{or} \quad S < 1 \tag{1}$$

is associated with the existence of expanding solutions, that is, waves with positive speeds. Theorem 4.6 proves that it is a necessary condition of the existence of such solutions. Numerical simulations confirm their existence (Fig 8). Note that the wave speeds for the two components of solutions are, in general, different from each other.
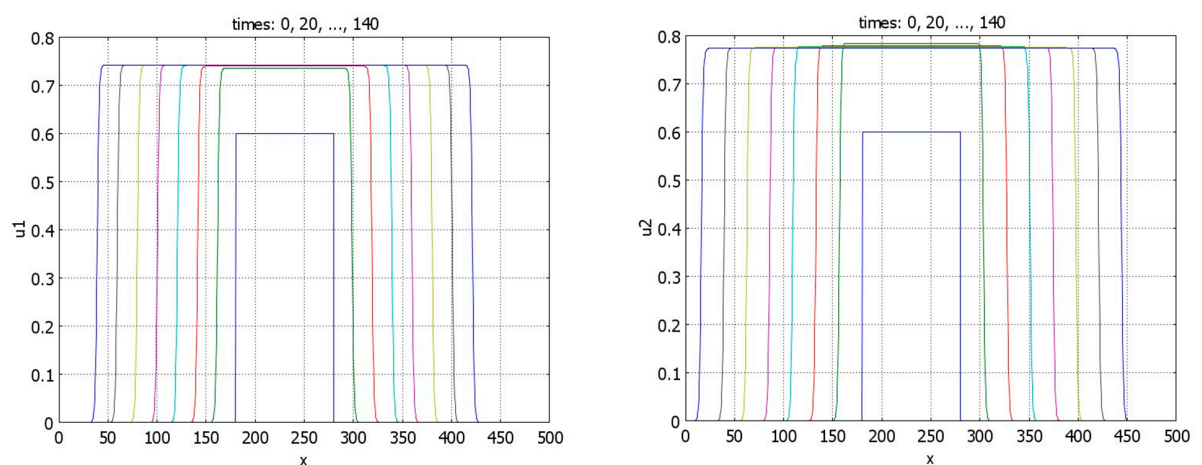
Fig 8. Time profiles of the function u_1 (left) and of the function u_2 (right) for $r_1 = s_1 = 0.5$, $r_2 = s_2 = 1.5$, $k_1 = 1.2$, $n_1 = 0.4$. The initial condition is a piece-wise constant function; $a_1 = a_2 = 1$, $b_1 = b_2 = 4$, $k_2 = 1$, $n_2 = 0.5$. For these values of parameters $p_* = q_* = 1.5$ and $S \approx 0.427$. Dynamics of solutions corresponds to expanding waves.

If inequality (1) is opposite and conditions of Theorem 3.5 are satisfied, then there exist stationary pulses (Fig 9). We note that the components u_1 and u_2 of solution of problem (4)-(6) are coupled only through the values of their integrals. Therefore, for any solution $u_1(x)$, $u_2(x)$ of this problem, then functions $u_1(x)$, $u_2(x+h)$ also satisfy it for any real h. This property is illustrated in Fig 9 (left). Increase of the value of k_1 decreases the component u_1 of the solution (Fig 9, right). It also leads to the decrease of u_2 through the integral $J(u_1)$.

Let us now consider the case $r_1 = s_1 = r_2 = s_2 = 0$ (cf. Proposition 4.4). If condition (1) is satisfied, then numerical simulations show that the stationary pulses are unstable, and we observe wave propagation (Fig 10). If inequality (1) is opposite, waves with negative speeds are observed (Fig 11). In agreement with Proposition 4.4, there are no stationary pulses.

Convergence of solution to a wide flat pulse is shown in Fig 12. In the beginning of simulation, solution resembles a travelling wave. After some time, it slows down and stops. Biologically, this example illustrates coordinated growth of two tissues to their final sizes. We use this example for numerical simulations of tissue regeneration. We cut the first tissue, while the second tissue is not changed. In the model, this means that we consider the initial condition with a partially truncated first component, while the initial condition for the second component represents the same stationary pulse as in the previous simulation. The solution of this problem converges to the same pulse solution. The integrals of the first and second components of the solution are shown in Fig 13. The integral of the first component monotonically converges to its stationary value, while the integral of the second component decreases in the beginning and grows later. This decrease in the beginning of simulations shows that the second tissue decreases its size to adjust to the first tissue.

5 Discussion

As indicated above in the introduction, tissue growth control can be influenced by tissue cross-talk and negative feedback. We will discuss here the biological mechanisms of this feedback and their realization in the model.
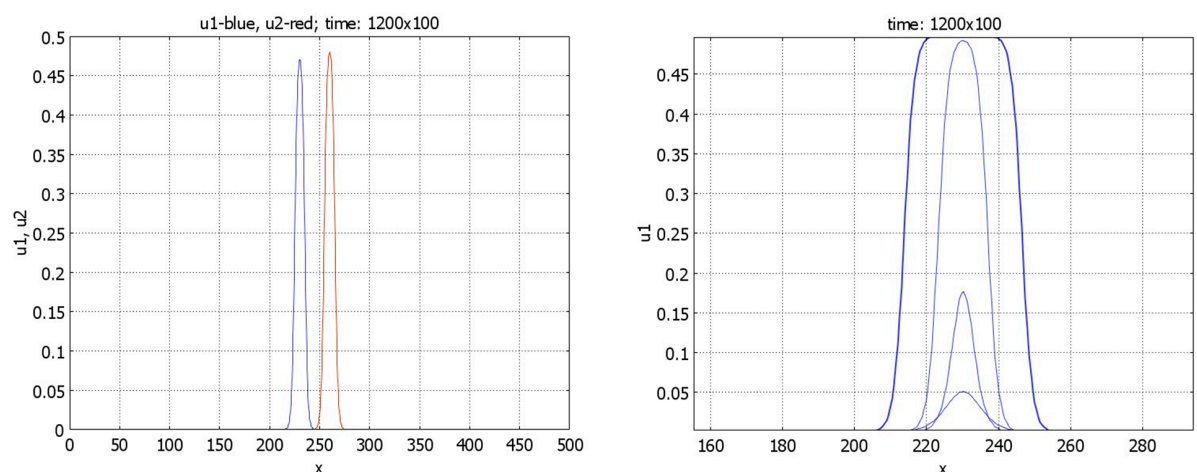
Fig 9. Left panel: profiles of the pulses u_1 and u_2 for $r_1 = s_1 = 0.5$, $r_2 = s_2 = 1.5$, $k_1 = 2$, $n_1 = 1$. The initial data for u_1 and u_2 are given by rectangles shifted by 30 space units. Right panel: profiles of the u_1 pulses for $r_1 = s_1 = 0.5$, $r_2 = s_2 = 1.5$, and fixed $n_1 = 2$. The maximal value of the profiles decreases with k_1 equal respectively to 0.75, 1, 2, 3. Other parameters: $a_1 = a_2 = 1$, $b_1 = b_2 = 4$, $k_2 = 1$, $n_2 = 0.5$, and $S \approx 1.78$.
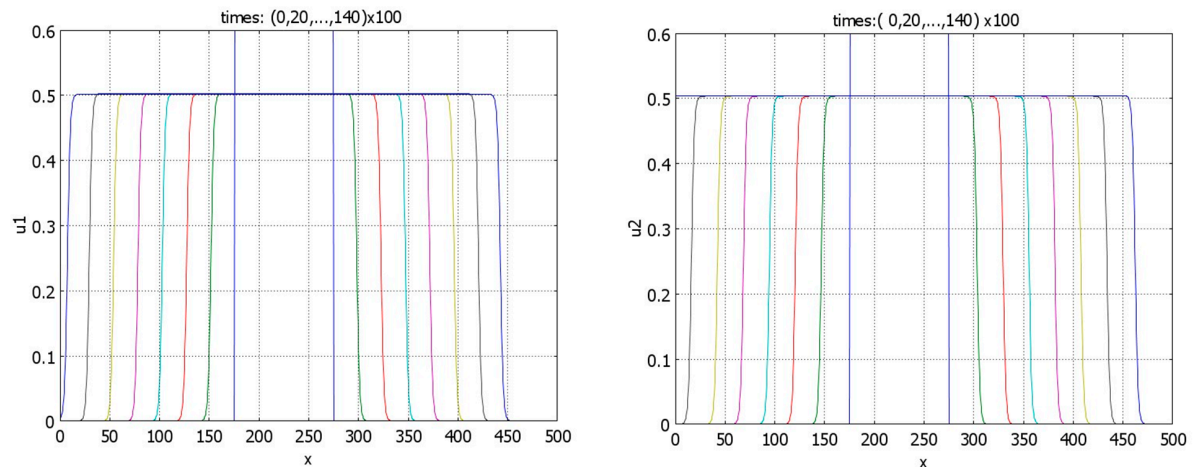
Fig 10. Time profiles of the function u_1 (left) and of the function u_2 (right) for $r_1 = s_1 = r_2 = s_2 = 0$, $k_1 = 1.6$, $n_1 = 0.7$, $k_2 = 1$, $n_2 = 0.5$. Other parameters: $a_1 = a_2 = 1$, $b_1 = b_2 = 4$. The initial conditions are given by piece-wise constant functions, $S \approx 0.996$.
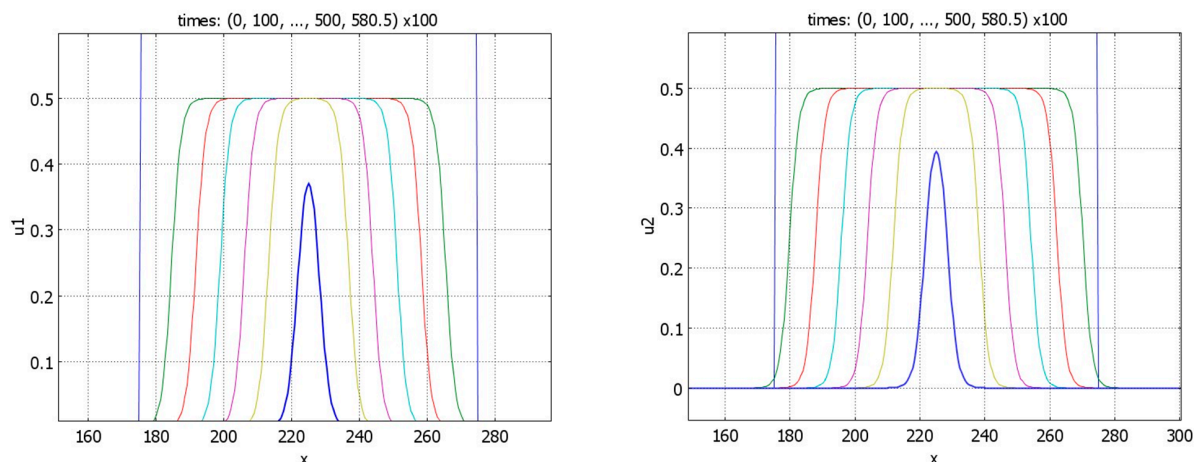
Fig 11. Time profiles of the function u_1 (left) and of the function u_2 (right) for $r_1 = s_1 = r_2 = s_2 = 0$, $k_1 = 1.67725$, $n_1 = 0.6709$. The initial condition is a piece-wise constant function. At time $t = 581 \cdot 100$ the functions $u_1(x, t)$ and $u_2(x, t)$ are point-wise smaller than 10^{-5}: the solution converges to zero. The values of parameters: $a_1 = a_2 = 1$, $b_1 = b_2 = 4$, $k_2 = 1$, $n_2 = 0.5$, $p_* = q_* = 1.5$, and $S \approx 1.00023$. In agreement with Proposition 4.4, no pulse solution is observed.

5.1 Chalones, growth-inhibitory feedback mechanisms, functional feedbacks

Chalones are tissue-specific, secreted factors that inhibit further cell proliferation in the tissue of origin. The concept of chalones originated with the hypothesis that organ size is regulated by locally produced substances that act to limit growth when a critical mass is achieved [64, 69]. Chalones are secreted in proportion to the size or cell number of the tissue. As the tissue grows, their concentration increases locally or systemically, inhibiting further proliferation.

Chalones are critical for maintaining tissue homeostasis and preventing excessive growth. The disruption of chalone signaling can result in unregulated tissue growth, contributing to tumorigenesis. For example, loss of myostatin expression in some cancers correlates with tumor progression and metastasis.
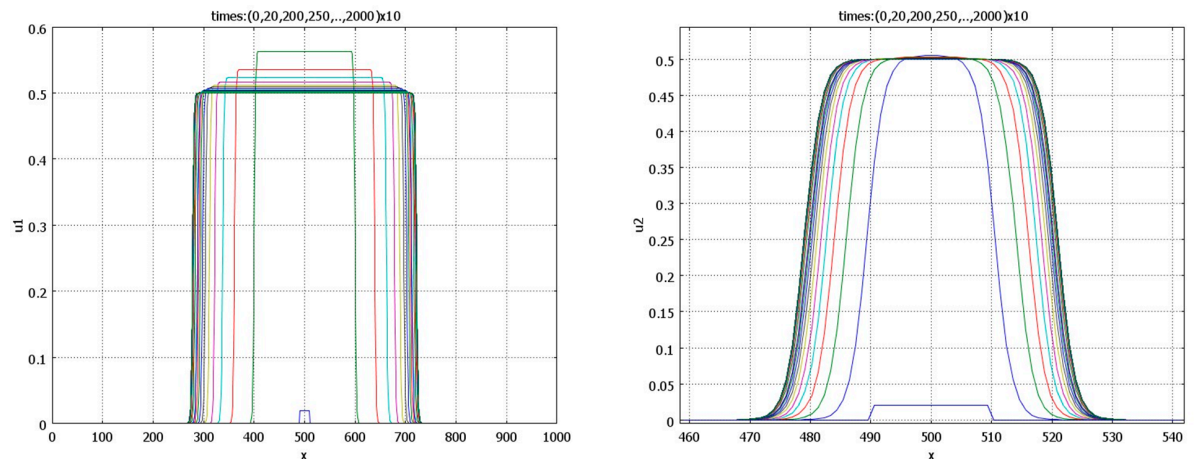
Fig 12. Time profiles of the function u_1 (left) and of the function u_2 (right) for $r_1 = 0.5, s_1 = 0.5, r_2 = 1.5, s_2 = 1.5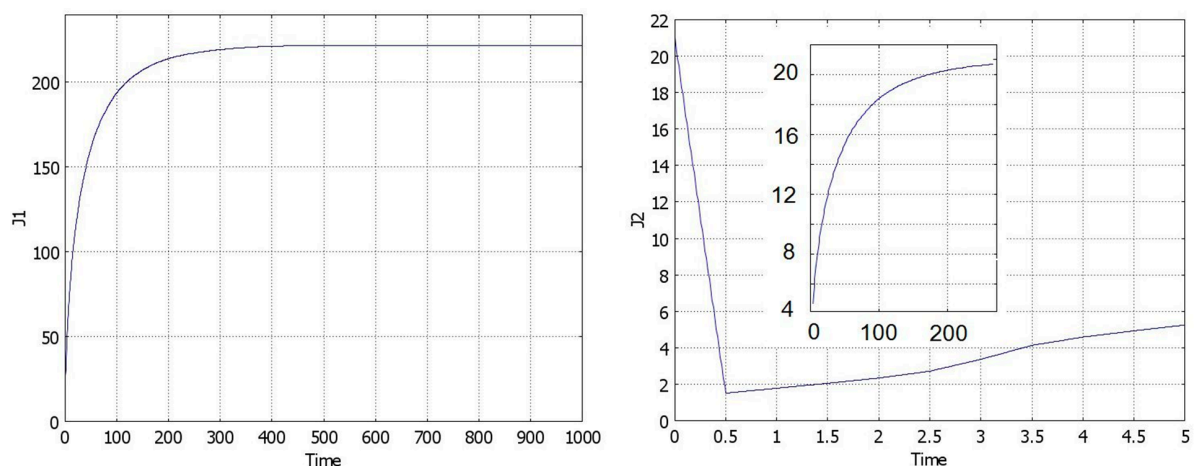, k_1 = 0.15, n_1 = 8$. The initial condition is a piece-wise constant function. Solution converges to the stable pulse. Note that the x-scales in the two figures are different. The values of parameters: $a_1 = a_2 = 1, b_1 = b_2 = 4, k_2 = 1, n_2 = 0.5, p_* = q_* = 1.5$, and $S \approx 1.067$.

https://doi.org/10.1371/journal.pone.0319120.g012

Fig 13. Integrals $J(u_1)$ (left) and $J(u_2)$ (right) in numerical simulations of tissue regeneration. For the same values of parameters as in Fig 12, the initial condition $u_1(x, 0)$ corresponds to the truncated stationary pulse, and for $u_2(x, 0)$ to the complete pulse. The solution converges to the same stationary pulse. The integral of the first component of the solution monotonically increases, while for the second component, it first decreases, then grows to its stationary value.

https://doi.org/10.1371/journal.pone.0319120.g013

The concept of chalones is being discussed during already more than a century with some examples and counter-examples (see the reviews in [2,64,70]). In the modern biological literature, it is accepted that it can work for some organs (see Table 1 in [69]), but it is not universal. Other mechanisms are also involved in tissue growth regulation depending on the tissue in question and physiological conditions (embryogenesis, development, trauma, neoplasia).

Growth is often regulated through negative feedback loops, which maintain a balance between proliferation and tissue size. These feedback loops can involve systemic signals (e.g., hormones) or local factors (e.g., chalones, mechanical stress).

Local feedback mechanisms include contact inhibition, where high cell density suppresses cell division, is a classic feedback mechanism. Mechanical cues, such as stiffness of the extracellular matrix (ECM), can signal cells to reduce proliferation as tissue tension increases. Molecules like FGF (fibroblast growth factors) and VEGF (vascular endothelial growth factor) operate in local feedback loops to regulate organ development and maintain proportions.

Parabiosis studies in mice (joining circulatory systems of two animals) have shown that systemic factors can rejuvenate aged tissues, but intrinsic local feedback mechanisms primarily govern growth control.

Another growth control is based on functional feedback mechanisms that use organ performance or output to regulate growth. Unlike chalones, which depend on mass or cell number, functional feedback ensures that tissue size matches physiological needs.

Examples of functional control include liver and bile acid flux. Bile acids synthesized by the liver are recirculated through the enterohepatic system. When bile acid flux increases due to enhanced digestion demands, hepatocyte proliferation is induced to expand liver size. Conversely, reduced bile acid flux signals that the liver has reached a sufficient size.

Another example concerns kidney and functional compensation. Following unilateral nephrectomy, the remaining kidney undergoes hypertrophy to compensate for lost function. The signal for this compensation may involve increased serum creatinine levels or local mechanical stress. Importantly, this compensatory growth primarily involves hypertrophy rather than hyperplasia. In thyroid and endocrine glands, negative feedback loops involving hormone levels (e.g., TSH and thyroid hormone) regulate the size and activity of endocrine organs. Hypothyroidism leads to compensatory thyroid hypertrophy (goiter), while hyperthyroidism suppresses TSH secretion, reducing thyroid size.

In distinction from chalones, functional feedback is performance-driven, whereas chalone mechanisms are based on physical size or cell number. Functional feedback often operates through systemic signaling, as seen in liver regeneration involving bile acids or kidney compensation mediated by metabolic demands.

5.2 Models of growth with negative feedbacks

The mechanisms of tissue growth control presented above act through negative feedback. Biological mechanisms of this feedback and their implementations in the models can be different. A common feature of these mechanisms, including functional feedback, is that there is some characterization of the tissue (signal, function) proportional to its size $J(u)$. If we denote its level by B, then we obtain Eq (3) for its time evolution.

From this point on, these mechanisms begin to differentiate. Global (systemic) feedback can be expressed by another signaling molecule C produced by some other organ and described by Eq (4). This endocrine signaling can up-regulate cell death in Eq (1) or down-regulate its proliferation.

Functional feedback, which is also systemic, is determined by some given value B_0 required by the organism. Therefore, tissue growth is proportional to $(B_0 - B)$ or, in the dimensionless form, to $(1-J(u))$ entering as a factor in the tissue proliferation rate. From the modelling point of view, this is similar to systemic feedback down-regulating cell proliferation in the previous paragraph.

Local (autocrine, paracrine) feedback, associated with chalones (though their action can also be systemic), decreases cell proliferation. However, the quantity of substance B with respect to a single tissue cell, that is $B/J(u)$ remains constant since $B \sim J(u)$. Therefore, its action does not depend on the tissue volume, and cannot control its growth.

There is a principal difference between the local feedback, where the *total* quantity of substance B is proportional to $J(u)$, and systemic feedback, where the *concentration* (level) of C in blood (or in the whole organism) is proportional to $J(u)$. In the first case, as discussed above, the quantity of B with respect to a single cell remains approximately constant, and feedback intensity does not depend on the tissue volume (Fig 14). But relative concentration of B can increase with time and act as growth inhibitor or growth promoter that decreases expression of their growth [69]. In the second case, depletion of C in the tissue is negligible compared to the whole organism, we do not divide C by $J(u)$. In this case, feedback intensity depends on the tissue volume $J(u)$.

Thus, we model systemic feedback, the mechanism of which can be related to chalones and to other negative feedbacks, or to the functional feedback.

5.3 Modelling results and biological interpretations

5.3.1 Single tissue with systemic feedback

Spatially-distributed solutions and tissue differentiation. The question of tissue differentiation in a growing embryo was first addressed by A. Turing in his seminal work [71]. He proposed a mechanism based on diffusion-driven instability, which arises from the interplay between long-range inhibition and short-range activation. This mechanism results in the formation of spatially periodic patterns. In spite of the enormous interest to Turing structures in mathematical biology, the mechanisms of cell differentiation in a growing embryo are likely to be different [72].

In Sect 3.1, we proposed an alternative mechanism for the emergence of spatial structures, which bifurcate from a spatially homogeneous solution. Biologically, this mechanism relies on local cell communication, which promotes cell proliferation, and global negative feedback, which stimulates cell death.

The global feedback operates through the integral term $J(u)$, which modifies the eigenvalue distribution of the linearized problem. Specifically, it decreases the eigenvalue λ_0 with the largest real part, as the corresponding eigenfunction ϕ_0 is a positive constant, and $J(\phi_0) > 0$. However, for all other eigenfunctions, $\phi_i(x) = \cos(\pi n x / L)$, the integral vanishes, leaving the
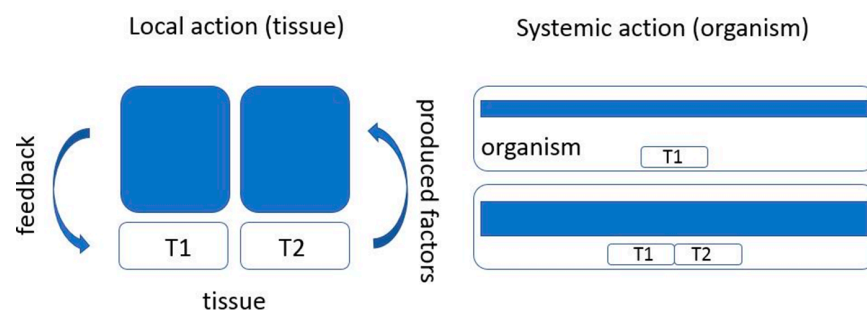
Fig 14. Local (left) and systemic (right) feedback on tissue growth by some factors produced by the tissue. In the local case, increasing the tissue twice ($T1 + T2$), increases the total amount of the produced factor. However, its amount with respect to the unit tissue volume remains the same. Therefore, local feedback cannot determine the tissue size. In systemic feedback, instead of the total amount of the produced factor in the whole organism, we measure its level (concentration). Increasing twice the tissue, we also increase twice this level. Its feedback on the unit tissue volume also increases.

eigenvalues unchanged. Consequently, under certain parameter conditions, the second eigenvalue λ_1 surpasses λ_0. This instability in the spatially homogeneous solution then leads to the formation of spatial structures.

A more detailed comparison between this instability and Turing instability is provided in [65], particularly regarding its dependence on interval length and the rates of cell division and death.

It is worth noting that in Eq (1), $u(x,t)$ is interpreted as cell concentration, with the diffusion term representing random cell motion. Alternatively, this variable can also be understood as the concentration of an autocrine signaling molecule or other locally produced molecules that regulate cell division or differentiation.

Existence of pulses. Spatially distributed solutions bifurcating from a constant solution take the form of pulses further into the instability region. This bifurcation occurs in problems defined on a bounded interval but not on the whole axis. On the whole axis, the integral of a positive constant solution is not defined, and for the zero solution, bifurcation does not occur. Therefore, in this context, we focus on the existence of pulses rather than their bifurcation.

The existence of pulses depends on the properties of the feedback function $g(J(u))$. Under the conditions specified in Theorem 3.2, Eq (12) admits a solution, which ensures the existence of a pulse. However, the uniqueness of this solution is not guaranteed by the theorem and may not generally hold. In the generic case, where solutions do not overlap, their number is odd. If the conditions on the feedback function are not met, the number of solutions becomes even, potentially resulting in no solutions at all. Notably, two pulse solutions were identified in [66] for a different function F in a population dynamics model.

One of the key conditions for the existence of pulses is $b>a$. Biologically, this implies that the effect of local cell-cell communication on the proliferation rate must be sufficiently strong. This phenomenon has some resemblance to the emergence of Turing structures, where short-range activation and long-range inhibition drive pattern formation. In this case, the long-range inhibition is provided by the negative feedback.

Stability of pulses. If $g(J(u)) \equiv$ const, that is, Eq (1) does not depend on the integral, then the pulse solution is unstable. Indeed, the eigenfunction of the zero eigenvalue of the corresponding eigenvalue problem is the derivative of the pulse solution. Therefore, it has variable sign. On the other hand, the eigenfunction corresponding to the eigenvalue with the maximal real part is positive [67]. Hence, $\lambda = 0$ is not the principal eigenvalue and, consequently, there is a positive eigenvalue. This means that the pulse solution is unstable.

Introduction of the integral term in the equation can make this solution stable (see also [73]). This is not proved mathematically but confirmed in numerical simulations. Stability of pulses can be related to existence and bifurcation of solutions of Eq (12).

Convergence to wide flat pulses is appropriate for tissue growth control. The solution dynamics looks like a wave propagation. After some time, its speed decreases and the propagation stops (Fig 6). This growth arrest is determined by the negative feedback through the tissue size $J(u)$.

It is important to note that such behavior of solution is observed for any small initial condition. Due to the time dependence of the integral $J(u)$, the nonlinearity in the equation is of the monostable type in the beginning of the simulation and of the bistable type some time later. This change in the type of equation provides growth of solution in the beginning and existence of a stable pulse for large time. From the biological point of view, this is appropriate for the description of tissue growth in embryogenesis, and in modelling of tumor growth.

5.3.2 Coordinated growth of two tissues. All tissues and organs in the growing organism precisely correspond to each other in their sizes and functionality. The question about the

mechanisms of this coordination is largely discussed in the biological literature (see the discussion above). In the model, tissue growth regulation is provided by a negative feedback by each tissue on itself, and by a positive feedback on the other one (see [64] for the biological discussion). The former controls tissue convergence to a final size (similar to the model of a single tissue), while the latter determines the proportional growth between the two tissues. The question about other possible models remains open. Note that for a model in population dynamics stable pulses can exist in the case where all interactions are negative [74].

In this work, we considered tissue cross-talk through the rate of cell death. Their interaction in the cell proliferation rate will be studied in the future works.

Existence of waves and pulses. Dynamics of solutions in the model of two tissue is determined by the parameter S which characterizes the feedback in the rate of cell death for both tissues. Larger values of this parameter correspond to stronger feedback. If $S>1$, then there exists a pulse solution (Theorem 4.5). Numerical simulations show that such solutions are stable. Thus, in the case of strong feedback, the final tissue sizes are finite.

Weak feedback in cell death corresponds to wave propagation (Theorem 4.6). In this case, existence of pulses is not observed in numerical simulations. We can conclude that weak feedback leads to the unlimited tissue growth.

Additional condition of the existence of pulses in Theorem 4.5, $r_1/r_2 < a_1$, $s_1/s_2 < a_2$, signify that in the beginning of tissue growth, when the feedback is negligible, the cell proliferation rate exceeds the death rate. Therefore, tissue growth can occur with any small initial condition. This corresponds to the biological understanding of this process.

An interesting case is provided by the conditions $r_1 = r_2 = s_1 = s_2 = 0$ which cannot be considered as a particular example of the more general case discussed above. This case is different from the point of view of the imposed conditions and of the corresponding results. The pulses can exist in this case but they are unstable, and wave propagation is observed in this case in numerical simulations.

Tissue growth rate. Tissue growth dynamics exhibit distinct phases: an initial exponential growth, a phase of constant growth, and a final phase of deceleration as the tissue stabilizes to its ultimate size [64,69]. These phases reflect both biological and model-based representations of tissue growth (Figs 5, 6, 13). Early exponential growth is driven by rapid cell proliferation, supported by abundant resources and minimal constraints. As cell density increases, however, growth transitions to a constant rate due to density-dependent inhibition of cell division. This phenomenon reflects contact inhibition and competition for limited resources, which collectively cap the proliferation rate. In the final phase, systemic feedback mechanisms come into play, curbing growth through the promotion of cell death or senescence. Negative feedback from systemic factors, such as signaling molecules or hormones, ensures that tissues do not exceed their optimal size, maintaining homeostasis.

In the modelling, the transition from the exponential growth to a constant growth rate occurs due to the logistic term in the proliferation rate. Instead of simultaneous cell division in the whole volume at the first stage, we observe predominant cell division at the exterior part of the tissue and lateral growth lile a reaction-diffusion wave. At the third stage, this propagation slows down and stops due to the integral term describing negative systemic feedback.

In regeneration, tissue growth dynamics involve additional complexities. When one tissue is ablated, compensatory mechanisms in the surrounding tissues are activated. These mechanisms often result in an initial decrease in the size of adjacent tissues, enabling proper recalibration and eventual size restoration [75] (cf. Fig 13). This decrease is thought to be regulated by systemic feedback that synchronizes growth rates across tissues, ensuring proportional

regeneration. The interplay of local cellular factors and systemic regulatory signals highlights the intricate control mechanisms underlying tissue growth and regeneration, providing insights into both normal development and potential therapeutic interventions. Understanding these processes is essential for unraveling the principles governing tissue homeostasis and recovery after injury.

6 Conclusions

This study presents a comprehensive mathematical framework for understanding tissue growth regulation via endocrine signaling. Through the development of reaction-diffusion models, we examined the interplay between local and systemic feedback mechanisms in controlling cell proliferation and tissue size. The models elucidate several critical phenomena, including:

Emergence of spatial structures. The analysis reveals that tissue growth and differentiation can be driven by local cell-cell communication, coupled with global feedback mechanisms. This combination leads to stationary pulse solutions, offering a novel explanation for tissue differentiation beyond classical Turing instability.

Regulation through negative feedback. The results highlight the importance of systemic feedback mechanisms, such as endocrine signaling, in stabilizing tissue growth and achieving proportionate sizes. Stability and existence of pulse solutions depend on the strength and type of feedback, with strong feedback ensuring finite tissue sizes, while weaker feedback leads to unlimited growth.

Coordinated growth of tissues. The study demonstrates that inter-tissue signaling can coordinate the growth of multiple tissues, ensuring harmonious development. Positive feedback between tissues amplifies this coordination, while negative feedback determines the final tissue size.

Bifurcation and stability of solutions. The existence and stability of stationary pulses and traveling wave solutions were characterized under various parameter regimes. These findings provide a mathematical basis for understanding phenomena such as growth arrest, regeneration, and tumor expansion.

Biological implications. The models suggested in this work offer insights into diverse biological processes, including embryogenesis, organ size regulation, and pathological conditions such as cancer. This framework also underscores the role of tissue cross-talk in maintaining systemic homeostasis.

Future work will extend these models to include additional biological complexities, such as functional feedback mechanisms and specific signaling pathways, to further enhance our understanding of growth regulation and tissue coordination.

Acknowledgments

Author contributions

Conceptualization: Vitaly Volpert.

Formal analysis: Vitaly Volpert.

Investigation: Bogdan Kazmierczak.

Software: Bogdan Kazmierczak.

Writing – original draft: Bogdan Kazmierczak, Vitaly Volpert.

Writing – review & editing: Bogdan Kazmierczak, Vitaly Volpert.

References

1. Pan D. The hippo signaling pathway in development and cancer. Dev Cell. 2010;19(4):491–505. https://doi.org/10.1016/j.devcel.2010.09.011 PMID: 20951342

2. Boulan L, Léopold P. What determines organ size during development and regeneration?. Development. 2021;148(1):dev196063. https://doi.org/10.1242/dev.196063 PMID: 33431590

3. Sun F, Poss KD. Inter-organ communication during tissue regeneration. Development. 2023;150(23):dev202166. https://doi.org/10.1242/dev.202166 PMID: 38010139

4. Hua H, Kong Q, Yin J, Zhang J, Jiang Y. Insulin-like growth factor receptor signaling in tumorigenesis and drug resistance: A challenge for cancer therapy. J Hematol Oncol. 2020;13(1):64. https://doi.org/10.1186/s13045-020-00904-3 PMID: 32493414

5. Viard I, Jaillard C, Saez JM. Regulation by growth factors (IGF-I, b-FGF and TGF-beta) of proto-oncogene mRNA, growth and differentiation of bovine adrenocortical fasciculata cells. FEBS Lett. 1993;328(1–2):94–8. https://doi.org/10.1016/0014-5793(93)80972-w PMID: 8344438

6. Mihai R. Physiology of the pituitary, thyroid, parathyroid and adrenal glands. Surgery (Oxford). 2014;32(10):504–12. https://doi.org/10.1016/j.mpsur.2014.07.008

7. Gutgesell HP, Rembold CM. Growth of the human heart relative to body surface area. Am J Cardiol. 1990;65(9):662–8. https://doi.org/10.1016/0002-9149(90)91048-b PMID: 2309636

8. Gilgenkrantz H, Collin de l'Hortet A. Understanding liver regeneration: From mechanisms to regenerative medicine. Am J Pathol. 2018;188(6):1316–27. https://doi.org/10.1016/j.ajpath.2018.03.008 PMID: 29673755

9. Yun YR, Won JE, Jeon E, Lee S, Kang W, Jo H, et al. Fibroblast growth factors: Biology, function, and application for tissue regeneration. J Tissue Eng. 2010;218142.

10. Bidlingmaier M, Strasburger CJ. Handbook of experimental pharmacology. 2010;195:187–200.

11. LeRoith D, Holly JMP, Forbes BE. Insulin-like growth factors: Ligands, binding proteins, and receptors. Mol Metab. 2021;52:101245. https://doi.org/10.1016/j.molmet.2021.101245 PMID: 33962049

12. Kumar MA, Baba SK, Sadida HQ, Marzooqi SA, Jerobin J, Altemani FH, et al. Extracellular vesicles as tools and targets in therapy for diseases. Signal Transduct Target Ther. 2024;9(1):27. https://doi.org/10.1038/s41392-024-01735-1 PMID: 38311623

13. Wynn TA, Vannella KM. Macrophages in tissue repair, regeneration, and fibrosis. Immunity. 2016;44(3):450–62. https://doi.org/10.1016/j.immuni.2016.02.015 PMID: 26982353

14. Bonewald L. Use it or lose it to age: A review of bone and muscle communication. Bone. 2019;120:212–8. https://doi.org/10.1016/j.bone.2018.11.002 PMID: 30408611

15. Stern JH, Rutkowski JM, Scherer PE. Adiponectin, leptin, and fatty acids in the maintenance of metabolic homeostasis through adipose tissue crosstalk. Cell Metab. 2016;23(5):770–84. https://doi.org/10.1016/j.cmet.2016.04.011 PMID: 27166942

16. Halbrook CJ, Pasca di Magliano M, Lyssiotis CA. Tumor cross-talk networks promote growth and support immune evasion in pancreatic cancer. Am J Physiol Gastrointest Liver Physiol. 2018;315(1):G27–35. https://doi.org/10.1152/ajpgi.00416.2017 PMID: 29543507

17. Leng G, MacGregor DJ. Models in neuroendocrinology. Math Biosci. 2018;305:29–41. https://doi.org/10.1016/j.mbs.2018.07.008 PMID: 30075152

18. Pattaranit R, van den Berg HA. Mathematical models of energy homeostasis. J R Soc Interface. 2008;5(27):1119–35. https://doi.org/10.1098/rsif.2008.0216 PMID: 18611843

19. Kim LU, D'Orsogna MR, Chou T. Onset, timing, and exposure therapy of stress disorders: Mechanistic insight from a mathematical model of oscillating neuroendocrine dynamics. Biol Direct. 2016;11(1):13. https://doi.org/10.1186/s13062-016-0117-6 PMID: 27013324

20. Zavala E, Wedgwood KCA, Voliotis M, Tabak J, Spiga F, Lightman SL, et al. Mathematical modelling of endocrine systems. Trends Endocrinol Metab. 2019;30(4):244–57. https://doi.org/10.1016/j.tem.2019.01.008 PMID: 30799185

21. WEISS P, KAVANAU JL. A model of growth and growth control in mathematical terms. J Gen Physiol. 1957;41(1):1–47. https://doi.org/10.1085/jgp.41.1.1 PMID: 13463267

22. Fischer MM, Herzel H, Blüthgen N. Mathematical modelling identifies conditions for maintaining and escaping feedback control in the intestinal epithelium. Sci Rep. 2022;12(1):5569. https://doi.org/10.1038/s41598-022-09202-z PMID: 35368028

23. Day SJ, Lawrence PA. Measuring dimensions: The regulation of size and shape. Development. 2000;127(14):2977–87. https://doi.org/10.1242/dev.127.14.2977 PMID: 10862736

24. Wartlick O, Mumcu P, Kicheva A, Bittig T, Seum C, Jülicher F, et al. Dynamics of Dpp signaling and proliferation control. Science. 2011;331(6021):1154–9. https://doi.org/10.1126/science.1200037 PMID: 21385708

25. Chara O, Tanaka EM, Brusch L. Mathematical modeling of regenerative processes. Curr Topics Dev Biol. 2014:283–317.

26. Murray JD. Mathematical biology II: Spatial models and biomedical applications. Third ed. Springer; 2003.

27. Mozokhina A, Ait Mahiout L, Volpert V. Modeling of viral infection with inflammation. Mathematics. 2023;11(19):4095. https://doi.org/10.3390/math11194095

28. Bessonov N, Neverova D, Popov V, Volpert V. Emergence and competition of virus variants in respiratory viral infections. Front Immunol. 2023;13:945228. https://doi.org/10.3389/fimmu.2022.945228 PMID: 37168105

29. Moussaoui A, Volpert V. The impact of immune cell interactions on virus quasi-species formation. Math Biosci Eng. 2024;21(11):7530–53. https://doi.org/10.3934/mbe.2024331 PMID: 39696850

30. Abercrombie M. Contact inhibition in tissue culture. In Vitro. 1970;6(2):128–42. https://doi.org/10.1007/BF02616114 PMID: 4943054

31. Folkman J, Hochberg M. Self-regulation of growth in three dimensions. J Exp Med. 1973;138(4):745–53. https://doi.org/10.1084/jem.138.4.745 PMID: 4744009

32. Freyer JP, Sutherland RM. Regulation of growth saturation and development of necrosis in EMT6/Ro multicellular spheroids by the glucose and oxygen supply. Cancer Res. 1986;46(7):3504–12. PMID: 3708582

33. Verhulst PF. Notice sur la loi que la population poursuit dans son accroissement. Correspondance mathematique et physique. 1838;10:113–21.

34. Sherratt JA, Murray JD. Models of epidermal wound healing. Proc Biol Sci. 1990;241(1300):29–36. https://doi.org/10.1098/rspb.1990.0061 PMID: 1978332

35. Gerlee P. The model muddle: In search of tumor growth laws. Cancer Res. 2013;73(8):2407–11. https://doi.org/10.1158/0008-5472.CAN-12-4355 PMID: 23393201

36. Sporn MB, Roberts AB. Autocrine growth factors and cancer. Nature. 1985;313(6005):745–7. https://doi.org/10.1038/313745a0 PMID: 3883191

37. Derynck R, Budi EH. Specificity, versatility, and control of TGF-β family signaling. Sci Signal. 2019;12(570):eaav5183. https://doi.org/10.1126/scisignal.aav5183 PMID: 30808818

38. Beck B, Blanpain C. Mechanisms regulating epidermal stem cells. EMBO J. 2012;31(9):2067–75. https://doi.org/10.1038/emboj.2012.67 PMID: 22433839

39. Byrne HM, Chaplain MAJ. Modelling the role of cell-cell adhesion in the growth and development of carcinomas. Math Comput Model. 1996;24(12):1–17. https://doi.org/10.1016/s0895-7177(96)00174-4

40. Galle J, Loeffler M, Drasdo D. Modeling the effect of deregulated proliferation and apoptosis on the growth dynamics of epithelial cell populations in vitro. Biophys J. 2005;88(1):62–75. https://doi.org/10.1529/biophysj.104.041459 PMID: 15475585

41. Marciniak-Czochra A. Receptor-based models with hysteresis for pattern formation in hydra. Math Biosci. 2006;199(1):97–119. https://doi.org/10.1016/j.mbs.2005.10.004 PMID: 16386765

42. Björnström L, Sjöberg M. Mechanisms of estrogen receptor signaling: Convergence of genomic and nongenomic actions on target genes. Mol Endocrinol. 2005;19(4):833–42. https://doi.org/10.1210/me.2004-0486 PMID: 15695368

43. Pollak M. Insulin and insulin-like growth factor signalling in neoplasia. Nat Rev Cancer. 2008;8(12):915–28. https://doi.org/10.1038/nrc2536 PMID: 19029956

44. Ashwell JD, Lu FW, Vacchio MS. Glucocorticoids in T cell development and function*. Annu Rev Immunol. 2000;18:309–45. https://doi.org/10.1146/annurev.immunol.18.1.309 PMID: 10837061

45. Denver RJ. The molecular basis of thyroid hormone-dependent central nervous system remodeling during amphibian metamorphosis. Comp Biochem Physiol C Pharmacol Toxicol Endocrinol. 1998;119(3):219–28. https://doi.org/10.1016/s0742-8413(98)00011-5 PMID: 9826995

46. Enderling H, Chaplain MAJ. Mathematical modeling of tumor growth and treatment. Curr Pharm Des. 2014;20(30):4934–40. https://doi.org/10.2174/1381612819666131125150434 PMID: 24283955

47. Deisboeck TS, Wang Z, Macklin P, Cristini V. Multiscale cancer modeling. Annu Rev Biomed Eng. 2011;13:127–55. https://doi.org/10.1146/annurev-bioeng-071910-124729 PMID: 21529163

48. Eymard N, Bessonov N, Gandrillon O, Koury MJ, Volpert V. The role of spatial organization of cells in erythropoiesis. J Math Biol. 2015;70(1–2):71–97. https://doi.org/10.1007/s00285-014-0758-y PMID: 24496930

49. Zaitseva NV, Kiryanov DA, Lanin DV, Chigvintsev VM. A mathematical model of the immune and neuroendocrine systems mutual regulation under the technogenic chemical factors impact. Comput Math Methods Med. 2014;2014:492489. https://doi.org/10.1155/2014/492489 PMID: 24872840

50. Fekete C, Lechan RM. Central regulation of hypothalamic-pituitary-thyroid axis under physiological and pathophysiological conditions. Endocr Rev. 2014;35(2):159–94. https://doi.org/10.1210/er.2013-1087 PMID: 24423980

51. Bernal J. Thyroid hormone receptors in brain development and function. Nat Clin Pract Endocrinol Metab. 2007;3(3):249–59. https://doi.org/10.1038/ncpendmet0424 PMID: 17315033

52. Haase VH. Regulation of erythropoiesis by hypoxia-inducible factors. Blood Rev. 2013;27(1):41–53. https://doi.org/10.1016/j.blre.2012.12.003 PMID: 23291219

53. Jelkmann W. Regulation of erythropoietin production. J Physiol. 2011;589(Pt 6):1251–8. https://doi.org/10.1113/jphysiol.2010.195057 PMID: 21078592

54. Kahn SE, Hull RL, Utzschneider KM. Mechanisms linking obesity to insulin resistance and type 2 diabetes. Nature. 2006;444(7121):840–6. https://doi.org/10.1038/nature05482 PMID: 17167471

55. Saltiel AR, Kahn CR. Insulin signalling and the regulation of glucose and lipid metabolism. Nature. 2001;414(6865):799–806. https://doi.org/10.1038/414799a PMID: 11742412

56. Quarles LD. Skeletal secretion of FGF-23 regulates phosphate and vitamin D metabolism. Nat Rev Endocrinol. 2012;8(5):276–86. https://doi.org/10.1038/nrendo.2011.218 PMID: 22249518

57. Razzaque MS. The FGF23-Klotho axis: Endocrine regulation of phosphate homeostasis. Nat Rev Endocrinol. 2009;5(11):611–9. https://doi.org/10.1038/nrendo.2009.196 PMID: 19844248

58. Pedersen BK, Febbraio MA. Muscles, exercise and obesity: Skeletal muscle as a secretory organ. Nat Rev Endocrinol. 2012;8(8):457–65. https://doi.org/10.1038/nrendo.2012.49 PMID: 22473333

59. Eckel J. Myokines in metabolic homeostasis and diabetes. Diabetologia. 2019;62(9):1523–8. https://doi.org/10.1007/s00125-019-4927-9 PMID: 31263909

60. Zeller R, López-Ríos J, Zuniga A. Vertebrate limb bud development: Moving towards integrative analysis of organogenesis. Nat Rev Genet. 2009;10(12):845–58. https://doi.org/10.1038/nrg2681 PMID: 19920852

61. Zaret KS. Genetic programming of liver and pancreas progenitors: Lessons for stem-cell differentiation. Nat Rev Genet. 2008;9(5):329–40. https://doi.org/10.1038/nrg2318 PMID: 18398419

62. Hanahan D, Coussens LM. Accessories to the crime: Functions of cells recruited to the tumor microenvironment. Cancer Cell. 2012;21(3):309–22. https://doi.org/10.1016/j.ccr.2012.02.022 PMID: 22439926

63. Zhang J, Niu C, Ye L, Huang H, He X, Tong W-G, et al. Identification of the haematopoietic stem cell niche and control of the niche size. Nature. 2003;425(6960):836–41. https://doi.org/10.1038/nature02041 PMID: 14574412

64. Simnett JD. Regulation of growth and cell division in the whole organism. Regulation of growth in neoplasia. Basel: Karger; 1981. p. 1–51.

65. Kazmierczak B, Volpert V. On a new mechanism of the emergence of spatial distributions in biological models. Appl Math Lett. 2025;163:109427. https://doi.org/10.1016/j.aml.2024.109427

66. Volpert V. Elliptic partial differential equations. Birkhauser; 2014.

67. Volpert AI, Volpert VA. Spectrum of elliptic operators and stability of travelling waves. Asymptotic Anal. 2000;23(2):111–34. https://doi.org/10.3233/asy-2000-392

68. Marion M, Volpert V. Existence of pulses for monotone reaction-diffusion systems. SIAM J Math Anal. 2023;55(2):603–27. https://doi.org/10.1137/21m1453219

69. Lui JC, Baron J. Mechanisms limiting body growth in mammals. Endocr Rev. 2011;32(3):422–40. https://doi.org/10.1210/er.2011-0001 PMID: 21441345

70. Elgjo K, Reichelt KL. Chalones: From aqueous extracts to oligopeptides. Cell Cycle. 2004;3(9):1208–11. https://doi.org/10.4161/cc.3.9.1087 PMID: 15326370

71. Turing AM. The chemical basis of morphogenesis. Philos Trans R Soc Lond B. 1952;237(641):37–72.

72. Shahbazi MN. Mechanisms of human embryo development: From cell fate to tissue shape and back. Development. 2020;147(14):dev190629. https://doi.org/10.1242/dev.190629 PMID: 32680920

73. Volpert V. Pulses and waves for a bistable nonlocal reaction–diffusion equation. Appl Math Lett. 2015;44:21–5. https://doi.org/10.1016/j.aml.2014.12.011

74. Volpert V, Reinberg N, Benmir M, Boujena S. On pulse solutions of a reaction–diffusion system in population dynamics. Nonlin Anal: Theory Meth Applic. 2015;120:76–85. https://doi.org/10.1016/j.na.2015.02.017

75. Lagasse E, Levin M. Future medicine: From molecular pathways to the collective intelligence of the body. Trends Mol Med. 2023;29(9):687–710. https://doi.org/10.1016/j.molmed.2023.06.007 PMID: 37481382